the same tissues, these findings suggest that the metabolism of IDL (VLDL remnant) and CR could be mediated by the VLDL receptor in peripheral fatty acid-active tissues, in concert with LPL (3).

Type III hyperlipoproteinemia is a genetic lipid disorder that is characterized by the accumulation of cholesterol-rich CR and hepatic β-VLDL. Most patients of type III hyperlipoproteinemia are homozygous for a mutant form of apoE (apoE2/2, Arg_{158}-Cys) that is not recognized by hepatic LDL receptors. We performed a competition study for binding with β-VLDL using VLDL derived from normolipidemic human subjects, homozygous for either apoE3/3 or apoE2/2, in LDL receptor-deficient CHO cells expressing the human VLDL receptor. In contrast to the LDL receptor, VLDL receptor bound apoE 2/2 VLDL or apoE 3/3 VLDL identically *in vitro* (24). Furthermore, adenovirus-mediated VLDL receptor expression in the liver of apoE2/2 and apoE3-Leiden transgenic mice lowered cholesterol levels, indicating that the VLDL receptor recognized apoE2/2 and apoE3-Leiden. The reduction in plasma cholesterol was mainly due to a reduction in the VLDL levels (25).

Lp (a) is a major inherited risk factor associated with premature heart disease and stroke. Strickland and colleagues (18) demonstrated that Lp (a) was recognized by the VLDL receptor, and clearance of Lp (a) was delayed in VLDL receptor-deficient mice. At the moment, the lipoproteins recognized by the VLDL receptor are VLDL, IDL (VLDL remnants), CR, and Lp (a).

Regulation of the VLDL receptor expression

When a cell takes up LDL particles into the cytoplasm through LDL receptor, three steps act to stabilize the cell's cholesterol content: (i) a suppression of 3-hydroxy-3-methylglutaryl coenzyme A (HMG-CoA) reductase gene (a key enzyme for de novo cholesterol synthesis) and acceleration of the degradation of the enzyme protein, (ii) an activation of Acyl-CoA: cholesterol acyltransferase (ACAT), a cholesterol-esterifying enzyme, to protect cells from free cholesterol, and (iii) a suppression of the LDL receptor own gene (a key lipoprotein receptor taking up plasma cholesterol). It has been accepted that the LDL receptor is down-regulated by intracellular lipoproteins. We first reported that the VLDL receptor is not down regulated by sterols in THP-1 and rabbit resident alveolar macrophages (9, 10). Western blots also showed that the LDL receptor protein disappeared when 100 μg/ml of β-VLDL was added to the medium for 48 hours, but the VLDL receptor protein level was not changed in THP-1 cells (Fig. 4). There is a sterol regulatory element (SRE)-1 in the human LDL receptor gene and two SRE-1-like sequences in the VLDL receptor gene (9). SRE-1 contains a direct repeat of the nucleotide sequence CAC on the same DNA strand, separated by two Cs. The two CAC sequences are considered to be the target of SRE-binding protein 1, which controls transcription of the LDL receptor gene. The SRE-1-like sequences in the VLDL receptor contain single nucleotide substitutions that disrupt the direct CAC repeats. This might be the reason why VLDL receptor expression is not regulated by intracellular lipoproteins.

In addition, a fasted state induced high VLDL receptor expression in the heart and low expression in the fat in mice, even though the expression in rats was not changed by a 48-hour fasting state (26, 27). We also confirmed that, in Balb/c mice fasted for 48 hours, VLDL receptor as well as LPL, fatty acid translocase (FAT)/CD36, heart-type fatty acid-binding protein (H-FABP), acyl-CoA synthetase (ACS) and long chain acyl-CoA dehydrogenase (LCAD) mRNAs, as fatty acid metabolism indicators, increased. Pyruvate kinase (PK) and glyceraldehyde-3-phosphate dehydrogenase (GAPDH) mRNAs, as glucose metabolism indicators, did not change. Electron microscopic examination indicated that the lipid droplets accumulated in the hearts of Balb/c mice fasted for 48 hours. During the development of SD (Sprague-Dawley) rats, VLDL receptor, LPL, FAT/CD36, H-FABP, ACS and LCAD mRNAs increased gradually with growth. However, PK and GAPDH mRNAs did not show this tendency. In cultured neonatal rat cardiomyocytes, VLDL receptor expression increased with days in culture, which was compatible with the *in vivo* results. Oil red-O staining showed cardiomyocytes after 7 days in culture (when the VLDL receptor protein is present) had accumulated β-VLDL. There were no detectable LDL receptor mRNAs in cultured neonatal rat cardiomyocytes, showing that remnant lipoproteins (β-VLDL) are taken up by the myocardium through the VLDL receptor (13). Triglyceride hydrolysis by LPL results in the generation of free fatty acids, 2-monoglycerol and remnant lipoprotein particles (IDL and CR). The resultant fatty acids are transported across the plasma membrane into the heart by simple

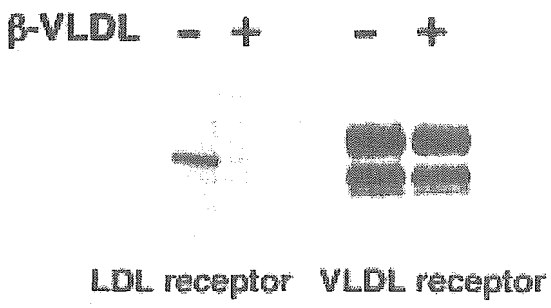

Fig. 4. Western blots study in THP-1 cells.
LDL receptor proteins virtually disappeared by the addition of β-VLDL (100 μg/ml) for 48 hours. VLDL receptor proteins remained.

diffusion and membrane-associated transporters (FAT/CD36, FATP and FABPpm). On the other hand, remnant lipoprotein particles are also taken up into the heart by the VLDL receptor.

Thyroid hormone was a positive regulator of the VLDL receptor in rat skeletal muscle but not in the fat or heart (27). VLDL receptor expression in rabbits is up-regulated by estrogen in the heart and down-regulated by granulocyte-macrophage colony-stimulating factor (GM-CSF) in muscle (28, 29). In JEG-3 and BeWo choriocarcinoma cells, two trophoblast-derived cell lines, 8-bromo-cAMP suppressed VLDL receptor expression. On the other hand, insulin and clofibrate (hypolipidemic drugs) up-regulated VLDL receptor expression. 25-hydroxycholesterol did not lead to sterol negative feedback on VLDL receptor expression (30). The VLDL receptor mRNA in adipose tissue and muscle was increased by 14-day gemfibrozil treatment in rabbits, indicating that the enhanced VLDL receptor expression was one of the mechanisms of the lipid-lowering effect of fibrate (31). IFN (Interferon)-γ inhibited VLDL receptor expression in PMA-treated THP-1 cells (monocytes), HL-60 cells and human monocyte-derived macrophages. However, this effect was not observed in normal THP-1 cells (12).

In contrast with the non-sterol regulation of VLDL receptor expression *in vitro*, Tiebel *et al.* (32) examined dietary regulation of the VLDL receptor in C57BL/6, LDL receptor knockout (LDL-R-/-), apoE knockout (apoE-/-) and LDL receptor/apoE double knockout (LDL-R-/-; apoE-/-) mice. VLDL receptor mRNA expression was down-regulated 3-fold by administrting an atherogenic diet, in the heart and skeletal muscle only, in LDL-R-/- mice. VLDL receptor mRNA was up-regulated by an atherogenic diet in the adipose tissue in all models except LDL-R-/-; apoE-/- mice. These findings suggest that SRE-1-like sequences in the VLDL receptor gene may be functional in the heart and skeletal muscle when LDL receptor is absent, and that apoE is required for regulation of VLDL receptor expression.

Reliable evidence of VLDL receptor as a lipoprotein receptor *in vivo*

In 1996, a conflicting report using VLDL receptor knockout (VLDL-R-/-) mice to study VLDL receptor as a lipoprotein receptor was published. VLDL-R-/- mice did not show any lipoprotein abnormality, although the adipose tissue mass of VLDL-R-/- mice was reduced (33). On the other hand, gene expression of the VLDL receptor in the liver declined plasma cholesterol levels in various laboratories (25, 34–36). We suggested that the tissue distribution of VLDL receptor might be a reason why VLDL receptor deficiency did not induce lipoprotein abnormality and why the plasma lipoprotein level was controlled by lipoprotein receptors in the liver. In 2000, Tacken *et al.* (37) elegantly solved this problem and demonstrated that the VLDL receptor is a peripheral lipoprotein receptor for VLDL triglycerides *in vivo*. They created VLDL receptor/LDL receptor double knockout (VLDL-R-/-; LDL-R-/-) mice and VLDL receptor over-expressing on LDL receptor knockout (LDL-R-/-) mice. When the mice were fed a high-fat diet, a lack of the VLDL receptor (VLDL-R-/-; LDL-R-/-) resulted in a significant increase in the serum triglyceride levels, and over expression of the VLDL-R resulted in a significant decrease in the serum triglyceride levels, compared to those in the LDL-R-/- mice. Furthermore, a period of prolonged fasting with a chow diet showed a significant increase in serum triglyceride levels in VLDL-R-/-; LDL-R-/- mice compared to those in LDL-R -/- mice. These data indicate that the plasma lipoprotein level in mice strongly depends on LDL receptor in the liver, and LDL receptor disguised the effect of VLDL receptor on lipoprotein metabolism.

Multiple Functions

Gene therapy for familial hypercholesterolemia and apoE mutants

The adenovirus-mediated transfer of the VLDL receptor gene into LDL receptor knockout mice liver greatly enhanced the ability to clear the IDL fraction, resulting in a marked lowering of the plasma IDL/LDL fraction (34, 35). Moreover, helper-dependent adenovirus-mediated delivery of VLDL receptor into hepatocytes produced the long-term lowering of plasma cholesterol and prevented atherosclerosis development in LDL receptor knockout mice (36). Gene therapy using VLDL receptor instead of LDL receptor for familial hypercholesterolemia (FH) is reasonable, because the normal LDL receptor might be recognized as a foreign protein in FH patients. VLDL receptor is non-immunogenic because it is normally expressed in fatty acid-active tissues, even in FH patients. Gene therapy using VLDL receptor has a possibile use in the treatment of apoE mutants, because VLDL receptor binds apoE2/2 and apoE3-Leiden (25). As yet there has been no report of gene therapy using VLDL receptor for human FH or apoE mutants.

Metabolic syndrome/atherosclerosis and the VLDL receptor

Metabolic syndrome is characterized by a cluster of obesity, insulin resistance, hypertension, and atherogenic dyslipidemia, and is associated with increased risk of coronary heart disease. It seems that VLDL receptor is involved in the mechanism of metabolic syndrome because VLDL receptor knockout (VLDL-R-/-) mice revealed a modest decrease in adipose tissue mass (33), and a higher affinity ligand of the VLDL receptor is remnant lipoprotein (3). Recently, Goudriaan *et al.* (38) reported that VLDL-R-/- mice remained lean and did not have insulin resistance after 17 weeks of a high-fat, high-calorie

(HFC) diet compared to wild-type mice, and the weight gain of VLDL-R-/- on ob/ob mice was less profound compared with that of ob/ob mice. Moreover, VLDL receptor deficiency led to increased plasma triglyceride after HFC feeding. These data indicated that inhibition of VLDL receptor expression in adipose tissue may be a therapeutic strategy for obesity.

VLDL receptor expression, primarily in macrophages, has been confirmed in human and rabbit atherosclerotic lesions (16–19). In addition, we reported that IFN-γ inhibited VLDL receptor expression and foam cell formation in three human macrophages (PMA-induced THP-1, PMA-induced HL-60 and human monocyte-derived macrophages) by β-VLDL, which is a representative lipoprotein in metabolic syndrome and type III hyperlipoproteinemia (12). These data showed that VLDL receptor might be a macrophage β-VLDL receptor, which is one of the receptors for macrophage foam cell formation. However, controversial findings using a mouse model *in vivo* have been reported. Yagyu *et al.* (39) showed that atherosclerosis was not different between HuB (human apo B) transgenic mice and VLDL receptor-deficient HuB transgenic mice after 4 months of an atherogenic diet. Tacken *et al.* (40) also showed that neither VLDL receptor deficiency nor endothelial VLDL receptor over expression affected the atherosclerotic lesion size. Interestingly, they indicated that deficiency for the VLDL receptor profoundly increased intimal thickening after vascular injury. We were not able to detect a sufficient amount of VLDL receptor expression in mouse peritoneal macrophages or J774 mouse macrophage cells (data not shown). At this time, we do not have any data to explain this difference between humans and mice.

Reelin signaling and the VLDL receptor

In 1999, we encountered an impact paper from Herz and colleagues (41) showing that the absence of both apoER2 and VLDL receptor in mice led to an inversion of cortical layers and the absence of cerebellar foliation. This phenotype is similar to that seen in animals carrying a mutation in either the reelin gene or the disabled-1 (Dab-1) gene. Both VLDL receptor and apoER2 can bind reelin on their extracellular domains, which subsequently induces the tyrosine phosphorylation of Dab-1 (42, 43). Dab-1 not only binds to the Asn-Pro-Xxx-Tyr (NPxY; where x denotes any amino acid) sequences in the cytoplasmic domain of both apoER2 and VLDL receptor, but also binds to those of the LDL receptor and LRP-1 (41). The NPVY sequence in LDL receptor has been accepted as a coated pit signal sequence, but these findings opened a new era of signaling research on the LDL receptor family (44).

Novel functions of VLDL receptor

In addition to apoE and LPL (7, 8, 22, 45), VLDL receptor binds receptor-associated protein (RAP) (46), thrombospondin-1 (47), urokinase plasminogen activator (uPA)/plasminogen activator inhibitor-1 complex (45, 48), several other proteinase-serpin complexes (49), and tissue factor pathway inhibitor (TFPI) (50). More recently, it has been reported that a 23-amino acid fragment of TFPI localized to the C-terminus mediated the VLDL receptor, and they showed that the VLDL receptor might be involved in angiogenesis and tumor growth (51). Early study using VLDL receptor-transfected COS-7 cells indicated that cell growth was inhibited by the VLDL receptor, and this growth inhibition was ligand-independent (52). VLDL receptor knockout mice were always segregated with the retinal angiogenesis and subretinal neovascularization (53). On the other hand, it seems that endothelial cells are important sites for VLDL receptor because the movement of active LPL across endothelial cells involves both heparan sulfate proteoglycan and VLDL receptor, and VLDL receptor knockout mice showed lower plasma LPL activity, though the exact mechanism is under investigation (37, 54).

Beyond the function of VLDL receptor as a peripheral lipoprotein receptor, the possibilities of its physiological function have been extended to include signal transduction, angiogenesis and tumor growth.

Acknowledgement: This research was supported in parts\ by research grants from the Ministry of Education, Culture, Sports, Science, and Technology of Japan.

References

(1) Brown MS and Goldstein JL: A receptor-mediated pathway for cholesterol homeostasis. Science, 232: 34–47, 1986

(2) Yamamoto T, Davis CG, Brown MS, Schneider WJ, Casey ML, Goldstein JL, and Russell DW: The human LDL receptor: A cysteine-rich protein with multiple Alu sequences in its mRNA. Cell, 39: 27–38, 1984

(3) Takahashi S, Sakai J, Fujino T, Miyamori I, and Yamamoto TT: The very low-density lipoprotein (VLDL) receptor. A peripheral lipoprotein receptor for remnant lipoproteins into fatty acid active tissues. Mol Cell Biochem, 248:121–127, 2003

(4) Herz J, Hamann U, Rogne S, Myklebost O, Gausepohl H, and Stanley KK: Surface location and high affinity for calcium of a 500-kd liver membrane protein closely related to the LDL-receptor suggest a physiological role as lipoprotein receptor. EMBO J, 7: 4119–4127, 1988

(5) Herz J and Strickland DK: LRP: a multifunctional scavenger and signaling receptor. J Clin Invest, 108: 779–784, 2001

(6) Herz J: LRP: a bright beacon at the blood-brain bar-

rier. J Clin Invest, 112: 1483–1485, 2003
(7) Takahashi S, Kawarabayasi Y, Nakai T, Sakai J, and Yamamoto T: Rabbit very low density lipoprotein receptor: A low density lipoprotein receptor-like protein with distinct ligand specificity. Proc Natl Acad Sci U S A, 89: 9252–9256, 1992
(8) Yamamoto T, Takahashi S, Sakai J, and Kawarabayasi Y: The very low density lipoprotein receptor-A second lipoprotein receptor that may mediate uptake of fatty acids into muscle and fat cells. Trends Cardiovasc Med, 3: 144–148, 1993
(9) Sakai J, Hoshino A, Takahashi S, Miura Y, Ishii H, Suzuki H, Kawarabayasi Y, and Yamamoto T: Structure, chromosome location, and expression of the human very low density lipoprotein receptor gene. J Biol Chem, 269: 2173–2182, 1994
(10) Suzuki J, Takahashi S, Oida K, Shimada A, Kohno M, Tamai T, Miyabo S, Yamamoto T, and Nakai T: Lipid accumulation and foam cell formation in Chinese hamster ovary cells overexpressing very low density lipoprotein receptor. Biochem Biophys Res Commun, 206: 835–842, 1995
(11) Kohno M, Takahashi S, Oida K, Suzuki J, Tamai T, Yamamoto T, and Nakai T: 1α, 25-dihydroxyvitamin D_3 induces VLDL receptor mRNA expression in HL-60 cells in association with monocytic differentiation. Atherosclerosis, 133: 45–49, 1997
(12) Kosaka S, Takahashi S, Masamura K, Kanehara H, Sakai J, Tohda G, Okada E, Oida K, Iwasaki T, Hattori H, Kodama T, Yamamoto T, and Miyamori I: Evidence of macrophage foam cell formation by very low density lipoprotein receptor: Interferon-γ inhibition of very low-density lipoprotein receptor expression and foam cell formation in macrophages. Circulation, 103: 1142–1147, 2001
(13) Kamataki A, Takahashi S, Masamura K, Iwasaki T, Hattori H, Naiki H, Yamada K, Suzuki J, Miyamori I, Sakai J, Fujino T, and Yamamoto TT: Remnant lipoprotein particles are taken up into myocardium through VLDL receptor. A possible mechanism for cardiac fatty acid metabolism. Biochem Biophys Res Commun, 293: 1007–1013, 2002
(14) Wyne KL, Pathak RK, Seabra MC, and Hobbs HH: Expression of the VLDL receptor in endothelial cells. Arterioscler Thromb Vasc Biol, 16: 407-415, 1996
(15) Magrané J, Reina M, Pagan R, Luna A, Casaroli-Marano RP, Angelin B, Gåfvels M, and Vilaró S: Bovine aortic endotherial cells express a variant of the very low density lipoprotein receptor that lacks the O-linked sugar domain. J Lipid Res, 39: 2172–2181, 1998
(16) Multhaupt HAB, Gåfvels ME, Kariko K, Jin H, Arenas-Elliott C, Goldman BI, Strauss-III JF, Angelin B, Warhol MJ, and McCrae KR: Expression of very low density lipoprotein receptor in the vascular wall. Am J Pathol, 148: 1985–1997,1996
(17) Nakazato K, Ishibashi T, Shindo J, Shiomi M, and Maruyama Y: Expression of very low density lipoprotein receptor mRNA in rabbit atherosclerotic lesions. Am J Pathol, 149: 1831–1838,1996
(18) Argraves KM, Kozarsky KF, Fallon JT, Harpel PC, and Strickland DK: The atherogenic lipoprotein Lp (a) is internalized and degraded in a process mediated by the VLDL receptor. J Clin Invest, 100: 2170–2181,1997
(19) Hiltunen TP, Luoma JS, Nikkari T, and Yla-Herttuala S: Expression of LDL receptor, VLDL receptor, LDL receptor-related protein, and scavenger receptor in rabbit atherosclerotic lesions. Marked induction of scavenger receptor and VLDL receptor expression during lesion development. Circulation, 97: 1079–1086,1998
(20) Christie RH, Chung H, Rebeck W, Strickland D, and Hyman BT: Expression of the very low-density lipoprotein receptor (VLDL-r), an apolipoprotein-E receptor, in the central nervous system and in Alzheimer's disease. J Neuropathol Exp Neurol, 55: 491–498, 1996
(21) Patel DD, Forder RA, Soutar AK, and Knight BL: Synthesis and properties of the very-low-density-lipoprotein receptor and a comparison with the low-density-lipoprotein receptor. Biochem J, 324: 371–377, 1997
(22) Takahashi S, Suzuki J, Kohno M, Oida K, Tamai T, Miyabo S, Yamamoto T, and Nakai T: Enhancement of the binding of triglyceride-rich lipoproteins to the very low density lipoprotein receptor by apolipoprotein E and lipoprotein lipase. J Biol Chem, 270: 15747–15754, 1995
(23) Niemeier A, Gåfvels M, Heeren J, Meyer N, Angelin B, and Beisiegel U: VLDL receptor mediates the uptake of human chylomicron remnants in vitro. J Lipid Res, 37: 1733–1742, 1996
(24) Takahashi S, Oida K, Ookubo M, Suzuki J, Kohno M, Murase T, Yamamoto T, and Nakai T: Very low density lipoprotein receptor binds apolipoprotein E2/2 as well as apolipoprotein E3/3. FEBS Lett, 386: 197–200, 1996
(25) van Dijk KW, van Vlijmen BJM, va der Zee A, van't Hof B, van der Boom H, Kobayashi K, Chan L, Havekes LM, and Hofker MH: Reversal of hypercholesterolemia in apolipoprotein E2 and apolipoprotein E3-Leiden transgenic mice by adenovirus-mediated gene transfer of the VLDL receptor. Arterioscler Thromb Vasc Biol, 18: 7–12, 1998
(26) Kwok S, Singh-Bist A, Natu V, and Kraemer FB: Dietary regulation of the very low density lipoprotein receptor in mouse heart and fat. Horm Metab Res, 29: 524–529, 1997

(27) Jokinen EV, Landschulz KT, Wyne KL, Ho YK, Frykman PK, and Hobbs HH: Regulation of the very low density lipoprotein receptor by thyroid hormone in rat skeletal muscle. J Biol Chem, 269, 26411–26418, 1994
(28) Masuzaki H, Jingami H, Yamamoto T, and Nakao K: Effects of estradiol on very low density lipoprotein receptor mRNA levels in rabbit heart. FEBS Lett, 347, 211–214, 1994
(29) Ishibashi T, Yokoyama K, Shindo J, Hamazaki Y, Endo Y, Sato T, Takahashi S, Kawarabayasi Y, Shiomi M, Yamamoto T, and Maruyama Y: Potent cholesterol-lowering effect by human granulocyte-macrophage colony-stimulating factor in rabbits: possible implications of enhancement of macrophage functions and an increase in mRNA for VLDLR. Arterioscler Thromb, 14, 1534–1541, 1994
(30) Wittmaack FM, Gåfvels ME, Bronner M, Matsuo H, McCrae KR, Tomaszewski JE, Robinson SL, Strickland DK, and Strauss III JF: Localization and regulation of the human very low density lipoprotein/apolipoprotein-E receptor: trophoblast expression predicts a role for the receptor in placental lipid transport. Endocrinology, 136: 340–348, 1995
(31) Matuoka N, Jingami H, Masuzaki H, Mizuno M, Nakaishi S, Suga J, Tanaka T, Yamamoto T, and Nakao K: Effects of gemfibrozil administration on very low density lipoprotein receptor mRNA levels in rabbits. Atherosclerosis, 126: 221–226, 1996
(32) Tiebel O, Oka K, Robinson K, Sullivan M, Martinez J, Nakamuta M, Ishimura-Oka K, and Chen L: Mouse very low-density lipoprotein receptor (VLDLR): gene structure, tissue-specific expression and dietary and developmental regulation. Atherosclerosis, 145: 239–251, 1999
(33) Frykman PK, Brown MS, Yamamoto T, Goldstein JL, and Herz J: Normal plasma lipoproteins and fertility in gene-targeted mice homozygous for a disruption in the gene encoding very low density lipoprotein receptor. Proc Natl Acad Sci U S A, 92: 8453–8457, 1995
(34) Kobayashi K, Oka K, Forte T, Ishida B, Teng B, Ishimura-Oka K, Nakamuta M, and Chan L: Reversal of hypercholesterolemia in low density lipoprotein receptor knockout mice by adenovirus-mediated gene transfer of the very low density lipoprotein receptor. J Biol Chem, 271: 6852–6860, 1996
(35) Kozarsky KF, Jooss K, Donahee M, Strauss III JF, and Wilson JM: Effective treatment of familial hypercholesterolaemia in the mouse model using adenovirus-mediated transfer of the VLDL receptor gene. Nat Genet, 13: 54–62, 1996
(36) Oka K, Pastore L, Kim I-H, Merched A, Nomura S, Lee H-J, Merched-Sauvage M, Arden-Riley C, Lee B, Finegold M, Beaudet A, and Chen L: Long-term stable correction of low-density lipoprotein receptor-deficient mice with a helper-dependent adenoviral vector expressing the very low-density lipoprotein receptor. Circulation, 103: 1274–1281, 2001
(37) Tacken PJ, Teusink B, Jong MC, Harats D, Havekes LM, van Dijk KW, and Hofker MH: LDL receptor deficiency unmaskes altered VLDL triglyceride metabolism in VLDL receptor transgenic and knockout mice. J Lipid Res, 41: 2055–2065, 2000
(38) Goudriaan, JR, Tacken, PJ, Dahlmans, VEH, Gijbels, MJJ, Van Dijk KW, Havekes LM, and Jong MC: Protection from obesity in mice lacking the VLDL receptor. Arterioscler Thromb Vasc Biol, 21: 1488–1493, 2001
(39) Yagyu H, Lutz EP, Kako Y, Marks S, Hu Y, Choi SY, Bensadoun A, and Goldberg IJ: Very low density lipoprotein (VLDL) receptor-deficient mice have reduced lipoprotein lipase activity. Possible causes of hypertriglyceridemia and reduced body mass with VLDL receptor deficiency. J Biol Chem, 277: 10037–10043, 2002
(40) Tacken PJ, Delsing DJM, Gijbels MJJ, Quax PHA, Havekes LM, Hofker MH, and van Dijk KW: VLDL receptor deficiency enhances intimal thickening after vascular injury but does not affect atherosclerotic lesion area. Atherosclerosis, 162: 103–110, 2002
(41) Trommsdorff M, Gotthardt M, Hiesberger T, Shelton J, Stockinger W, Nimpf J, Hammer RE, Richardson JA, and Herz J: Reeler/Disabled-like disruption of neuronal migration in knockout mice lacking the VLDL receptor and apoE receptor 2. Cell, 97: 689–701, 1999
(42) D'Arcangelo G, Homayouni R, Keshvara L, Rice DS, Sheldon M, and Curran T: Reelin is a ligand for lipoprotein receptors. Neuron, 24: 471–479, 1999
(43) Hiesberger T, Trommsdorff M, Howell BW, Goffinet A, Mumby MC, Cooper JA, and Herz J: Direct binding of Reelin to VLDL receptor and apoE receptor 2 induces tyrosine phosphorylation of Disabled-1 and modulates Tau phosphorylation. Neuron, 24: 481–489, 1999
(44) Chen W-J, Goldstein JL, and Brown MS: NPXY, a sequence often found in cytoplasmic tails, is required for coated pit-mediated internalization of the low density lipoprotein receptor. J Biol Chem, 265: 3116–3123, 1990
(45) Argraves KM, Battey FD, MacCalman CD, McCrae KR, Gåfvels M, Kozarsky KF, Chappell DA, Strauss III JF, and Strickland DK: The very low density lipoprotein receptor mediates the cellular catabolism of lipoprotein lipase and urokinase-plasminogen activator inhibitor type I complexes. J Biol Chem, 270: 26550–26557, 1995
(46) Battey FD, Gåfvels ME, FitzGerald DJ, Argraves WS,

Chappell DA, Strauss III JF, and Strickland DK: The 39-kDa receptor-associated protein regulates ligand binding by the very low density lipoprotein receptor. J Biol Chem, 269: 23268–23273, 1994

(47) Mikhailenko I, Krylov D, Argraves M, Roberts DD, Liau G, and Strickland DK: Cellular internalization and degradation of thrombospondin-1 is mediated by the amino-terminal heparin binding domain (HBD). High affinity interaction of dimeric HBD with the low density lipoprotein receptor-related protein. J Biol Chem, 272: 6784–6791, 1997

(48) Heegaaed CW, Simonsen ACW, Oka K, Kjøller L, Christensen A, Madsen B, Ellgaard L, Chan L, and Andreasen PA: Very low density lipoprotein receptor binds and mediates endocytosis of urokinase-type plasminogen activator-type-1 plasminogen activator inhibitor complex. J Biol Chem, 270: 20855–20861, 1995

(49) Kasza A, Petersen HH, Heegaard CW, Oka K, Christensen A, Dubin A, Chan L, and Andreasen PA: Specificity of serine protease/serpin complex binding to very-low-density lipoprotein receptor and α_2-macroglobulin receptor/low-density-lipoprotein-receptor-related protein. Eur J Biochem, 248: 270–281, 1997

(50) Hembrough TA, Ruiz JF, Parathanassiu AE, Green SJ, and Strickland DK: Tissue factor pathway inhibitor inhibits endothelial cell proliferation via association with the very low density lipoprotein receptor. J Biol Chem, 276: 12241–12248, 2001

(51) Hembrough TA, Ruiz JF, Swerdlow BM, Swartz GM, Hammers HJ, Zhang L, Plum SM, Williams MS, Strickland DK, and Pribluda VS: Identification and characterization of a very low density lipoprotein receptor binding peptide from tissue factor pathway inhibitor that has antitumor and antiangiogenic activity. Blood, 103: 3374–3380, 2004

(52) Wada Y, Homma Y, Nakazato K, Ishibashi T, and Maruyama Y: Effect of overexpression of very low density lipoprotein receptor on cell growth. Heart Vessels, 15, 74–80, 2000

(53) Heckenlively JR, Hawes NL, Friedlander M, Nusinowitz S, Hurd R, Davisson M, and Chang B: Mouse model of subretinal neovascularization with choroidal anastomosis. Retina, 23: 518–522, 2003

(54) Obunike JC, Lutz EP, Li Z, Paka L, Katopodis T, Strickland DK, Kozarsky KF, Pillarisetti S, and Goldberg IR: Transcytosis of lipoprotein lipase across cultured endothelial cells both heparan sulfate proteoglycan and the very low density lipoprotein receptor. J Biol Chem, 276: 8934–8941, 2001

THE JOURNAL OF BIOLOGICAL CHEMISTRY
Vol. 279, No. 17, Issue of April 23, pp. 16954–16962, 2004
Printed in U.S.A.

A Krüppel-like factor KLF15 Contributes Fasting-induced Transcriptional Activation of Mitochondrial Acetyl-CoA Synthetase Gene *AceCS2**

Received for publication, November 4, 2003, and in revised form, February 4, 2004
Published, JBC Papers in Press, February 10, 2004, DOI 10.1074/jbc.M312079200

Joji Yamamoto,[a,b] Yukio Ikeda,[a,b] Haruhisa Iguchi,[b] Takahiro Fujino,[c] Toshiya Tanaka,[d] Hiroshi Asaba,[d] Satoshi Iwasaki,[b] Ryoichi X. Ioka,[b] Izumi W. Kaneko,[c] Kenta Magoori,[d] Sadao Takahashi,[e] Toshiyuki Mori,[f] Hiroshi Sakaue,[f] Tatsuhiko Kodama,[d] Masashi Yanagisawa,[b,g,h] Tokuo T. Yamamoto,[c] Sadayoshi Ito,[a] and Juro Sakai[b,d,i]

From the [a]Division of Nephrology, Endocrinology, and Vascular Medicine, Department of Medicine, the Tohoku University Graduate School of Medicine, Sendai 980-8574, Japan, the [b]Yanagisawa Orphan Receptor Project, Exploratory Research for Advanced Technology, Japan Science and Technology Corporation, Tokyo 135-0064, Japan, the [c]Tohoku University Gene Research Center, Sendai 981-8555, Japan, the [d]Laboratory for Systems Biology and Medicine, Research Center for Advanced Science and Technology, University of Tokyo, Tokyo 153-8904, Japan, the [e]Third Department of Internal Medicine, Fukui Medical University, Fukui, 910-1193, Japan, the [f]Division of Diabetes and Digestive and Kidney Diseases, Department of Clinical Molecular Medicine, Kobe University Graduate School of Medicine, Kobe 650-0017, Japan, and the [g]Howard Hughes Medical Institute, Department of Molecular Genetics, University of Texas Southwestern Medical Center at Dallas, Dallas, Texas 75235-9050

Acetyl-CoA synthetase 2 (AceCS2) produces acetyl-CoA for oxidation through the citric acid cycle in the mitochondrial matrix. AceCS2 is highly expressed in the skeletal muscle and is robustly induced by fasting. Quantification of AceCS2 transcripts both in C2C12 and human myotubes indicated that fasting-induced *AceCS2* gene expression appears to be independent on insulin action. Characterization of 5′-flanking region of the mouse *AceCS2* gene demonstrates that Krüppel-like factor 15 (KLF15) plays a key role in the trans-activation of the *AceCS2* gene. Deletion and mutation analyses of *AceCS2* promoter region revealed that the most proximal KLF site is a curtail site for the trans-activation of the *AceCS2* gene by KLF15. Using Sp-null *Drosophila* SL2 cells, we showed that the combination of KLF15 and Sp1 resulted in a synergistic activation of the *AceCS2* promoter. Mutation analyses of three GC-boxes in the *AceCS2* promoter indicated that the GC-box, located 8 bases downstream of the most proximal KLF15 site, is the most important GC-box in the synergistic trans-activation of the *AceCS2* gene by KLF15 and Sp1. GST pull-down assays showed that KLF15 interacts with Sp1 *in vitro*. Quantification of various KLF transcripts revealed that 48 h fasting robustly induced the KLF15 transcripts in the skeletal muscle. Together with the trans-activation of the *AceCS2* promoter, it is suggested that fasting-induced AceCS2 expression is largely contributed by KLF15. Furthermore, KLF15 overexpression induced the levels of AceCS2 transcripts both in myoblasts and in myotubes, indicating that *AceCS2* gene expression *in vivo* is indeed induced by KLF15.

Acetyl-CoA is an important intermediate in various metabolic pathways including fatty acid and cholesterol biosynthesis and the energy production by the citric acid cycle. There are several enzymes that generate acetyl-CoA in the mammals, including pyruvate dehydrogenase, which converts pyruvate to acetyl-CoA without generating free acetate. The degradation of fatty acid via β-oxidation system also produces acetyl-CoA as an end product. Although acetate is not an essential source of acetyl-CoA in animals, the enzymatic ligation for the production of acetyl-CoA from acetate and CoA is a key reaction in the catabolism of acetate formed by several conditions including bacterial fermentation in the colon, oxidation of ingested ethanol in the liver. Acetyl-CoA synthetase (AceCS,[1] EC 6.2.1.1) is an enzyme that catalyzes the production of acetyl-CoA from acetate and CoA. In particular, this enzyme plays a key role in the nervous system for recycling of acetate released by acetylcholine esterase for the formation and release of acetylcholine in cholinergic nerve terminals.

There are two AceCSs with similar enzymatic properties in mammals: one designated AceCS1 is a cytosolic enzyme and the other, designated AceCS2, is a mitochondrial matrix enzyme (1). Localized in the cytoplasm, AceCS1 provides acetyl-CoA for the synthesis of fatty acids and cholesterol. In contrast, AceCS2 produces acetyl-CoA for oxidation through the citric acid cycle to produce ATP and CO_2 in the mitochondrial matrix.

* This work was supported through Special Coordination Funds for Promoting Science and Technology from the Ministry of Education, Culture, Sports, Science and Technology of the Japanese Government, and Exploratory Research for Advanced Technology/ Japan Science and Technology Corporation (Yanagisawa orphan receptor project). The costs of publication of this article were defrayed in part by the payment of page charges. This article must therefore be hereby marked "*advertisement*" in accordance with 18 U.S.C. Section 1734 solely to indicate this fact.

[h] An Investigator of the Howard Hughes Medical Institute.

[i] To whom correspondence should be addressed: Laboratory for Systems Biology and Medicine, Research Center for Advanced Science and Technology, University of Tokyo, Tokyo 153-8904, Japan. Tel.: 81-3-5452-5472; Fax: 81-3-5452-5429; E-mail: jmsakai-tky@umin.ac.jp.

[1] The abbreviations used are: AceCS, acetyl coenzyme A synthetase; AFX, ALL1-fused gene from X chromosome; CMV, cytomegalovirus; FKHR, forkhead box O1a; GFP, green fluorescent protein; GLUT4, glucose transporter 4; GST, glutathione *S*-transferase; HSkMC, human skeletal muscle cell; HNF, hepatocyte nuclear factor; KLF, Krüppel-like factor; MEF2, myocyte enhancer factor 2; PGC-1α, peroxisome proliferator-activated receptor γ coactivator-1α; PPAR, peroxisome proliferator-activated receptor; RACE, rapid amplification of cDNA end; SREBP, sterol regulatory element-binding protein; DMEM, Dulbecco's modified Eagle's medium; EMSA, electrophoretic mobility shift assay; GFP, green fluorescent protein.

TABLE I
Primers for quantitative real-time RT-PCR

Gene	Sequence of forward and reverse primers (5′-3′)	Accession no.
Cyclophilin	CAAAGACACCAATGGCTCACAG CCACATCCATGCCCTCTAGAA	M60456
Human GAPDH	GCCATCAATGACCCCTTCATT TCTCGCTCCTGGAAGATGG	NM_002046
AceCS2	TCGTTCATACACAGGCAGGCTAT ACACGAGCTTGTGCGTCATG	NM_080575
Human AceCS2	GAGGATCAGAGGCCACATTTTT CACAGGAGAAACACTCACCAGG	NM_032501
Hexokinase II	CCTGCTTATTCACGGAGCTCA ATACTGGTCAACCTTCTGCACTTG	NM_013820
PDK4	GTGAACACTCCTTCGGTGCA TCAGGCTCTGGATATACCAGCTC	NM_013743
GLUT4	GACCTGTAACTTCATTGTCGGCA ATAGCATCCGCAACATACTGGA	NM_009204
KLF1	CTGACCAGAAGACCATACAAAGGA TGAGGACATGTGAGGTTTGTCC	NM_010635
KLF2	AGAATGCACCTGAGCCTGCTAG AATTTCCCCGAAAGCCTGC	ENSMUST00000006440
KLF3	CACCCCCTTTAATGAACCCAG TGGTTCTCTTGC AACAAGGCT	NM_008453
KLF4	CACAGGCGAGAAACCTTACCA AATTTCCACCCACAGCCGT	NM_010637
KLF5	TTCCAAACTGGCGATTCACAA ATTAACTGGCAGAGTGGCAGGTAA	NM_009769
KLF6	CCGGTGCCAAGCCTTTTAA GGTCAGACCTGGAGAAACACCT	NM_011803
KLF7	GTTTTGCACGGAGCGATGA AGACCTGGAGAAACACCTGTCG	NM_033563
KLF8	CTGTCCCACTCATTGGAGGAGA CAACTTTGACCGATCCAGCACT	XM_142240
KLF9	ATACAGGTGAACGGCCCTTTC TCCGAGCGCGAGAACTTTT	NM_010638
KLF10	TTCTCTCCAGCAAGCTTCGGA TCACTCTGCTCAGCTTTGTCCC	NM_013692
KLF11	CCCACCTTAAAGCTCATCTTCG GCAGGTAAAAGGCTTCTCCCCT	AK084913
KLF12	CAGTCAGTGCCGGTTGTCTACA CTCCATTTGTGCTTTGCCATG	NM_010636
KLF13	CCTCACCCCTTTGGTAATAGGA GCTGTGGACTTCTCAAGTTCGC	NM_021366
KLF14	CAGAGCTGGATGGCATAGAGGA TGAAAGGAGCGGCTAGCTCTT	AJ275988
KLF15	ACCGAAATGCTCAGTGGGTTACCTA GGAACAGAAGGCTTGCGAGTCA	NM_023184
KLF16	TGAGTTTGGCCTTTGTGGCAT TGTTCCCAATCCTGGAGTCCA	NM_078477

AceCS1 is a member of a family of genes whose transcription is regulated by sterol regulatory element-binding proteins (SREBPs), a basic helix-loop-helix leucine zipper transcription factor that activates multiple genes for cholesterol and fatty acid metabolism (2, 3). The levels of AceCS1 mRNA was induced when cultured cells were deprived of sterols and negatively regulated by sterol addition. In our previous study, we have shown that the *AceCS1* promoter region consists of multiple clustered SREBP binding sites and immediately downstream from this region there is a cluster of multiple GC-boxes (3). All these SREBP binding sites are bound with purified SREBP-1a and are required for a maximal response to cotransfected SREBP. The sterol regulation of the *AceCS1* gene was critically dependent on three closely spaced SREBP binding sites and an adjacent GC-box. We also showed that SREBP synergistically activated the *AceCS1* promoter along with Sp1 or Sp3 but not with nuclear factor Y (NF-Y).

AceCS2 is highly expressed in the cardiac and skeletal muscle and its regulation is completely different from that of AceCS1. A marked induction of AceCS2 mRNA is seen in the heart and skeletal muscle when animals are fasted (1). The levels of AceCS2 mRNA in the skeletal muscle of Zucker diabetic fatty rats were also increased compared with those in the normal littermates. These data indicated that the AceCS2 transcripts are induced in the heart and skeletal muscle under ketogenic conditions including prolonged fasting and diabetes.

During fasting, the expression of more than 94% of genes is not altered in the skeletal muscle. Among genes that are differentially expressed during fasting, genes involved in protein breakdown (components of the ubiquitin-proteasome pathway), fatty acid oxidation, and pyruvate dehydrogenase kinase 4 (PDK4) that suppresses glucose oxidation by inhibiting pyruvate dehydrogenase complex activity, are up-regulated (4, 5). In contrast, genes encoding glycolytic enzymes are down-regulated by fasting. Induction of genes involved in fatty acid oxidation is also seen in the skeletal muscle of diabetic mice (6). Although these changes indicate a complex adaptive program for sparing glucose, the mechanism underlining transcriptional regulation is not fully understood.

To define the mechanism of transcriptional induction of AceCS2 by fasting, we isolated and characterized 5′-flanking region of the mouse *AceCS2* gene. In this article, we describe that fasting induced transcriptional activation of the *AceCS2* gene in the skeletal muscle is largely contributed by a unique transcription factor, KLF15, a Krüppel-like factor. Our current data indicate a unique role of KLF15 in the activation of genes induced by prolonged fasting.

EXPERIMENTAL PROCEDURES

Materials—We obtained mouse Genome Walker kits and luminescent β-galactosidase reporter system from Clontech; the dual luciferase reporter assay system, pGL3 Basic, pRL-TK, and TNT Quick Coupled Transcription/Translation system from Promega Inc.; pcDNA3, pcDNA3.1, TOPO TA Cloning™ kit, TRIzol™ reagent, SuperScript II™, GeneRacer™ kit, LipofectAMINE PLUS, Dulbecco's modified Eagle's medium (DMEM), and Schneider's medium from Invitrogen; [γ-^{32}P]ATP (6000 Ci/mmol), and L-[^{35}S]methionine (1000 Ci/mmol), GST Gene Fusion System and Bulk GST Purification Module from Amersham Biosciences; QuikChange™ site-directed mutagenesis kit and MBS mammalian transfection kit from Stratagene; Oligotex-dT30 mRNA purification kit from TaKaRa (Shiga, Japan); nuclear extract kit from Active Motif (Carlsbad, CA); anti-human KLF15 polyclonal antibody from Abcam (catalog no. ab2647; Cambridge, UK); and oligonucleotides from Qiagen. Unless otherwise indicated, all restriction and DNA-modifying enzymes were obtained from Toyobo (Tokyo, Japan).

Expression Plasmids—To create a KLF15 expression plasmid, a full-length cDNA for rat KLF15 (provided by Dr. R. Hiramatsu, Genomics Science Laboratories, Sumitomo Pharmaceuticals Co. Ltd., Takarazuka, Japan) was inserted into pcDNA3. We obtained pcDNA1 vector-based plasmids for human MEF2A, mouse MEF2B, mouse MEF2C, and mouse MEF2D from Dr. E. N. Olson (Department of Molecular Biology, University of Texas Southwestern Medical Center) (7, 8); pSV-SPORT-PGC-1α, an SV40-driven plasmid containing mouse PGC-1α from Dr. B. M. Spiegelman (Dana-Farber Cancer Institute and the Department of Cell Biology, Harvard Medical School) (9); pcDNA3-based plasmid for mouse forkhead box O1a (FKHR) and mouse ALL1-fused gene from X chromosome (AFX), and pIRS-MLP-luc, a luciferase reporter plasmid driven by a promoter consisting of three tandem copies of a insulin responsive sequence (IRS) plus the adenovirus major late promoter (MLP) from Dr. A. Fukamizu (Center of Tsukuba Advanced Research Alliance, Institute of Applied Biochemistry, University of Tsukuba) (10, 11); pcDNA3.1-based plasmid for human c-Ets-1 from Dr. T. Minami (Laboratory for Systems Biology and Medicine, University of Tokyo, Japan) (12); and pcDNA3-based plasmids for mouse hepatic nuclear factor 1α (HNF1α) and mouse hepatocyte nuclear factor 1β (HNF1β) from Dr. K. Yamagata (Second Department of Internal Medicine, Osaka University Medical School, Suita, Japan) (13, 14). pCMV-MyoD, a CMV-driven plasmid for mouse MyoD, was constructed inserting the reverse transcription-PCR products of C2C12 myotube RNA into the pcDNA3 vector. pPac, a *Drosophila* actin 5C promoter-driven expression vector, pPacβ-gal containing an *Escherichia coli* β-galactosidase, and pPacSp1 and pPacSp3, respectively, containing Sp1 and Sp3, were provided by Dr. G. Suske (Philipps-Universität Marburg, Germany). pPac-based plasmid encoding rat KLF15 was generated by inserting the KLF15 cDNA into the pPac vector. An Sp1-GST fusion construct, pGEX-Sp1, was prepared by inserting the Sp1 cDNA fragment into the XhoI site of pGEX-4T-2.

Cloning of 5′-Flanking Region of Mouse AceCS2 Gene—The 5′-flanking region of the mouse *AceCS2* gene was cloned by PCR using Mouse Genome Walker kits (Clontech) as described previously (3). Briefly, the first PCR was conducted with adaptor primer 1 (provided by the supplier) and AceCS2 primer 1 (5′-TGACCACCCCGATTGTCCAGAG-3′) on a mouse genomic library (provided by the supplier). Nested PCR was then carried out with adaptor primer 2 (provided by the supplier) and AceCS2 primer 2 (5′-CGCAGCAGTCGCCCCACACCGCTGC-3′) on the first PCR products. The resulting 2.4-kb PCR product was subcloned into the pGEM-T easy cloning vector (Promega) to create pGEM-5′FL-AceCS2. Sequencing of the insert of pGEM-5′FL-AceCS2 was performed in both directions by the PCR cycle sequence method with an automatic sequence analyzer (Beckman Coulter CEQ 2000XL DNA Analysis System).

Rapid Amplification of cDNA End (RACE)—5′-RACE was performed using GeneRacer™ Kit (Invitrogen) according to the manufacturer's protocol. Briefly, 750 ng of poly(A)$^+$ RNA from quadriceps muscles of fasted mice was first treated with calf intestinal phosphatase to remove the 5′-phosphates. This eliminates truncated mRNA and non-mRNA from subsequent ligation with the GeneRacer™ RNA Oligo. The dephosphorylated RNA was then treated with tobacco acid pyrophosphatase to remove the 5′ cap structure from intact, full-length mRNA, and was ligated with 0.25 μg of the GeneRacer™ RNA Oligo using T4 RNA ligase at 37 °C for 1 h. The resulting products were then hybridized with random hexamer, reverse transcribed with SuperScript II reverse transcriptase, and subjected to PCR with a primer specific for the RNA Oligo (5′-CGACTGGAGCACGAGGACACTGA-3′) and an AceCS2 specific antisense primer (5′-CTGCACATGCTGATCCAGGCAGTTGA-3′). PCR parameters were 94 °C for 30 s and 68 °C for 1 min for 35 cycles. A major product of ~400 bp was cloned into the pCR2.1 vector (Invitrogen): eleven clones were isolated for sequencing analysis.

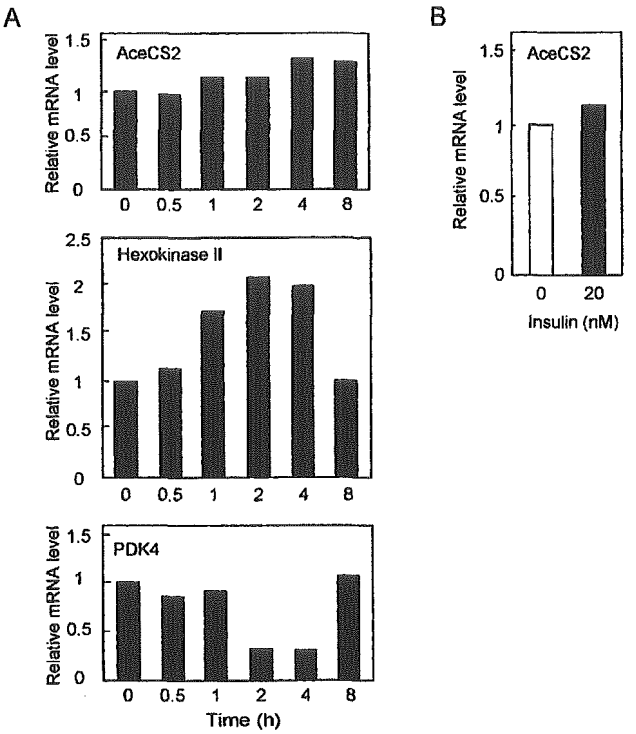

FIG. 1. **Effects of insulin on the levels of AceCS2 transcripts in cultured myotubes.** On day 0, C2C12 cells (*A*) and HSkMCs (*B*) were plated in 6-well plates at a density of 1 × 10^5 cells/well and grown in medium A. On day 2, cells were induced to differentiate into myotubes by incubating in medium B. Medium was changed every other day. On day 6, medium B was replaced by serum-free DMEM supplemented with 0.1% horse serum, 100 units/ml penicillin, and 100 μg/ml of streptomycin sulfate. C2C12 myotubes were treated with 200 nM bovine insulin for the indicated time periods (*A*), and human myotubes (HSkMCs) were cultured in the absence or presence of 20 nM bovine insulin for 16 h (*B*). Total RNA from C2C12 and human myotubes (*A* and *B*) were extracted, reverse-transcribed, and subjected to quantitative real time PCR as described under "Experimental Procedures." The levels of AceCS2, Hexokinase II, and PDK4 mRNA treated with insulin are shown in *panel A*. AceCS2 mRNA levels in HSkMCs cultured in the absence or presence of 20 nM bovine insulin are compared in *panel B*. Mouse cyclophilin or human GAPDH mRNA was used as the invariant control. Values represent the amount of mRNA in insulin-treated cells relative to that in the cells incubated without insulin, which is arbitrarily defined as 1.

AceCS2 Promoter-Reporter Constructs—pAceCS2(2347) is the mouse *AceCS2* promoter-luciferase reporter gene that spans −2347 to −1 relative to translation initiation site. pAceCS2(1928), pAceCS2(1528), pAceCS2(1383), pAceCS2 (940), pAceCS2 (654), pAceCS2 (110), and pAceCS2 (77), are 5′-deletion mutants of pAceCS2(2347), each contains a deletion with the 5′-end denoted in each parentheses and the same 3′-end point at −1. pAceCS2(2347) was constructed by PCR of pGEM-5′FL-AceCS2 using a forward primer starting from −2347 and a reverse primer OGY3as (5′-CTCGCCCGACGCCCCACGCG-3′). The PCR product was cloned into the SmaI site of pGL3 basic. pAceCS2(1928), pAceCS2(1528), pAceCS2(1383), pAceCS2 (940), pAceCS2 (654), pAceCS2 (110), and pAceCS2 (77) were constructed in a similar manner to pAceCS2(2347) using respective forward primers starting from the position −1928, −1528, −1383, −940, −654, −110, and −77, respectively, and coupled with a common reverse primer OGY3as. Base substitution mutants were generated in pAceCS2(1928) and pAceCS2 (654) using the QuikChange™ site-directed mutagenesis kit (Stratagene) according to the manufacturer's protocol. Oligonucleotides designed to mutate each element were as follows: the KLF site at −91, GGGTGGTG → GCTGCAGG; GC-box A at −132, AGGGCAGGC → AGACTAGTC; GC-box B at −76, GGGGCGGAG → GGAATTCAG; and GC-box C at −65, GGGGCGGGG → GGATATCGG.

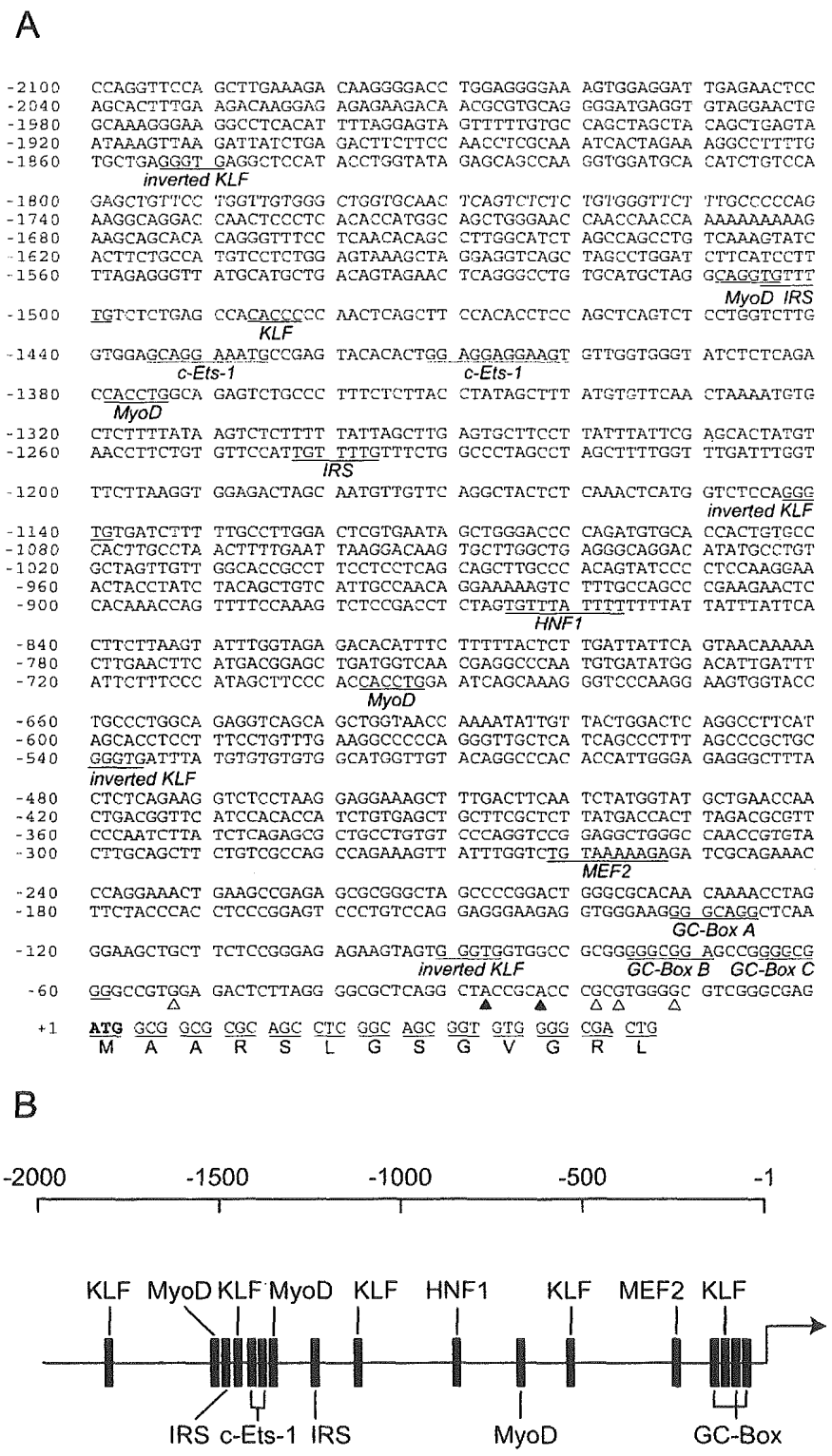

FIG. 2. **Mouse *AceCS2* Promoter.** *A*, nucleotide sequence of the 5′-flanking region of the mouse *AceCS2* gene. Nucleotide position +1 is assigned to the A of the ATG initiator codon (*boldface*), and the residues preceding it are indicated by *negative numbers*. The major and minor transcription initiation sites determined by 5′-RACE are indicated by *closed* and *open triangles*, respectively. Potential sites for KLF, MyoD, IRS, c-Ets-1, HNF1, MEF2, and GC-boxes are *underlined*. *B*, schematic diagram of the mouse *AceCS2* promoter. Potential elements are indicated by *closed boxes* and *labeled*.

Cells, Cell Culture, and Transfection—HEK293 cells (a line of human embryonic kidney cells) and C2C12 cells (a line of mouse myogenic cells) were obtained from Cell Resource Center for Biomedical Research at Tohoku University (Sendai, Japan). HSkMC (human skeletal muscle cells isolated from limbal skeletal muscle) were purchased from CELL APPLICATIONS, Inc. (San Diego, CA). HEK293 cells were maintained in medium A (DMEM containing 100 units/ml penicillin and 100 μg/ml of streptomycin sulfate, supplemented with 10% fetal bovine serum) at 37 °C in 5% CO_2. C2C12 cells and HSkMC were maintained in medium A and differentiated into myotubes in medium B (DMEM containing 100 units/ml penicillin, 100 μg/ml of streptomycin sulfate and 2% horse serum) for 5 days.

Schneider line 2 (SL2) cells, an Sp-null *Drosophila* cell line, were purchased from Invitrogen, maintained in Schneider's medium containing 100 units/ml penicillin and 100 μg/ml streptomycin sulfate, supplemented with 10% fetal bovine serum, and grown at 23 °C.

HEK293 and SL2 cells were transfected in 24-well plates using LipofectAMINE PLUS as described previously (15). After 24 h, the cells

were lysed with 0.1 ml of 1× passive lysis buffer (Promega), and aliquots were used for the measurement of firefly and *Renilla* luciferase activities as described below.

C2C12 cells were transfected exactly by the same method as that for HEK293 cells, except that the medium was switched to the differentiation medium (medium B) at 24 h post-transfection. After an additional incubation for 48 h, the cells were lysed and subjected to firefly and *Renilla* luciferase assays.

Enzyme Assays—Firefly and *Renilla* luciferase activities were measured according to the manufacturer's recommended protocol. Luciferase activities were determined in a Berthold Lumat Flash & Glow LB 955 luminometer. Firefly luciferase activities (relative light unit) were normalized by *Renilla* luciferase activities (relative light unit). For SL2 cells, β-galactosidase activities were determined using Luminescent β-galactosidase Reporter System (Clontech) and luciferase activities were normalized by the β-galactosidase activities (relative light unit).

Retroviral Vectors and Infection—The plat-E retroviral packaging cell line (16), and the retroviral vector pWZL containing the blasticidin S resistance gene were, respectively, provided by Drs. T. Kitamura (University of Tokyo, Tokyo, Japan) and G. P. Nolan (Stanford University, Palo Alto, CA). KLF15 cDNA was subcloned into the retrovirus vector, pWZL, to generate pWZL-KLF15.

To generate C2C12 cells stably expressing KLF15, the cells were infected with the retroviral vectors pWZL-KLF15 as described by Pear *et al.* (17) with the following modifications: Plat-E packaging cells were infected with plasmids using FuGENE 6 (Roche Applied Science) according to the manufacturer's instructions. After 24 h, cells were refed with fresh medium and cultured for an additional 24 h to obtain retroviral supernatants. For retroviral infection, C2C12 cells (50~60% confluence) were incubated with retroviral supernatants in the presence of 8 μg/ml polybrene for 24 h. Cells expressing KLF15 were selected for resistance to blasticidin S hydrochloride (10 μg/ml, Calbiochem, La Jolla, CA) and maintained in medium A. C2C12 cells stably expressing green fluorescent protein (GFP) were generated using a retrovirus vector encoding GFP (pWZL-GFP) and designated as C2C12/GFP.

Animal Manipulation—Male ICR mice were purchased from CLEA Japan, Inc (Tokyo, Japan). The mice were housed in a temperature- and humidity-controlled (26.5 °C and 35%, respectively) facility with a 12 h light/dark cycle (dark cycle was between 20.00–8.00). Mice were allowed to free access of water and a normal chow diet (CE-2, CLEA Japan) before experiments. Mice (7–8 weeks of age) were randomly divided into two groups: one group was fed *ad libitum* with regular diet and the other group was fasted for 48 h. All mice were sacrificed at the same time between 9.00 and11.00 AM. Quadriceps muscles were removed, weighed, and immediately frozen in liquid nitrogen and stored at −80 °C until RNA was extracted.

Quantitative Real Time PCR—First strand cDNA was synthesized from 5 μg of total RNA and oligo(dT) primers using SuperScript II reverse transcriptase. Specific primers for each gene transcript (listed in Table I) were designed using the Primer Express software (Applied Biosystems). Real time PCR contained, in a final volume of 20 μl, 3.125 ng of reverse-transcribed RNA, 167 nM of each primer, and 10 μl of 2× SYBR Green PCR Master Mix (catalog no. 4309155; Applied Biosystems). PCR was carried out in 384-well plates using the ABI PRISM 7900HT Sequence Detection System (Applied Biosystems). All reactions were performed in triplicate. The relative amounts of each transcript were calculated using the comparative C_T method (18). Mouse cyclophilin or human GAPDH mRNA was used as the invariant control.

Preparation of Nuclear Extracts and Electrophoretic Mobility Shift Assay (EMSA)—For EMSA, nuclear extracts from C2C12 cells stably expressing KLF15 were prepared using Nuclear Extract Kit (Active Motif) according to the manufacturer's protocol. Complementary single-stranded oligonucleotides corresponding to nucleotides −70 to −105 were annealed and end-labeled with [γ-^{32}P]ATP and T4 polynucleotide kinase. The labeled probe was incubated with 10 μg of nuclear extracts in a binding buffer containing 22.5 mM Hepes-KOH, pH 7.9, 2.6 mM $MgCl_2$, 13.3% glycerol, 50 mM KCl, 0.125 mM EDTA, 0.5 mM dithiothreitol, and 0.5 mg/ml poly(dI-dC) for 30 min at room temperature. For competition experiments, excess (100-fold) unlabeled double-stranded oligonucleotide was added to the binding mixture. In the supershift experiment, an antibody for KLF15 (2.5 μg) was added to the binding reaction. Protein-DNA complexes were analyzed by electrophoresis on 6% polyacrylamide gels as described previously (3).

GST Pull-down Analysis—^{35}S-labeled KLF15 was synthesized *in vitro* using pCMV-KLF15, TNT Quick Coupled Transcription/Translation system (Promega) and L-[^{35}S]methionine (Amersham Biosciences) according to the manufacturer's protocol. GST-Sp1 fusion protein was synthesized by the GST Gene Fusion System (Amersham Biosciences) and purified by the Bulk GST Purification Module (Amersham Biosciences). GST-Sp1 fusion protein and GST expressed in *E. coli* DH5α were isolated by using glutathione-Sepharose 4B beads. The immobilized GST protein beads were washed with phosphate-buffered saline and incubated with ^{35}S-labeled KLF15 at 4 °C for 1 h in the binding buffer (20 mM Hepes, pH 7.7, 75 mM KCl, 0.1 mM EDTA, 2.5 mM $MgCl_2$, 0.05% Nonidet P-40, 2 mM dithiothreitol, and 10% glycerol). The beads were washed seven times with the same buffer, and subjected to SDS-polyacrylamide gel electrophoresis and autoradiography.

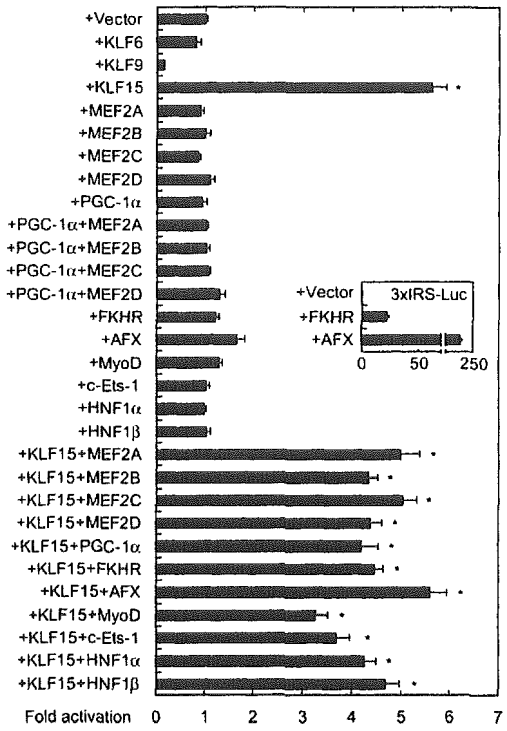

FIG. 3. **Trans-activation of *AceCS2* promoter by KLF15.** On day 0, HEK293 cells were plated at a density of 2 × 10^4 cells/well in 24-well plates. On day 1, the cells were transfected with 0.8 μg of pAceCS2(2347) along with 0.01 μg of the indicated expression plasmid(s). To normalize transfection efficiency, *Renilla* luciferase reporter (pRL-TK, 0.1 μg) was also included. On day 3, the cells were harvested for measurement of firefly and *Renilla* luciferase activities. *Renilla* luciferase activity was used as the internal reference to normalize transfection efficiency. The value for pAceCS2(2347)-luciferase activity co-transfected with pcDNA3.1 empty vector was arbitrarily set as 1. The -fold activation (luciferase activity co-transfected with each expression plasmid *versus* pcDNA3.1) is shown. The *error bars* represent mean ± S.E. of triplicate incubations. *Inset*, HEK293 cells were transfected with either 0.01 μg of pcDNA3.1 empty vector, pCMV-FKHR, or pCMV-AFX together with 0.8 μg of pIRS-luc-MLP and 0.1 μg of pRL-TK, and firefly and *Renilla* luciferase activities were determined as described above.

RESULTS

Effects of Insulin on Levels of AceCS2 Transcripts in Skeletal Muscle—We previously showed that fasting robustly increases the levels of AceCS2 mRNA in the skeletal muscle. There are several known fasting-inducible genes that are negatively regulated by insulin (19). These include genes encoding phosphoenolpyruvate carboxykinase (20), insulin-like growth factor-binding protein-1 (20), insulin receptor substrate-2 (21), and aquaporin adipose (22). To determine whether insulin negatively regulates the expression of AceCS2, we used C2C12 and human myotubes. As a positive control for the insulin response in C2C12 myotubes, we have analyzed the mRNA levels of two well known insulin responsive genes, hexokinase II and PDK4: hexokinase II and PDK4 are, respectively, up- and down-regulated by insulin. Cells were incubated with or without insulin for various time periods and the levels of AceCS2, hexokinase

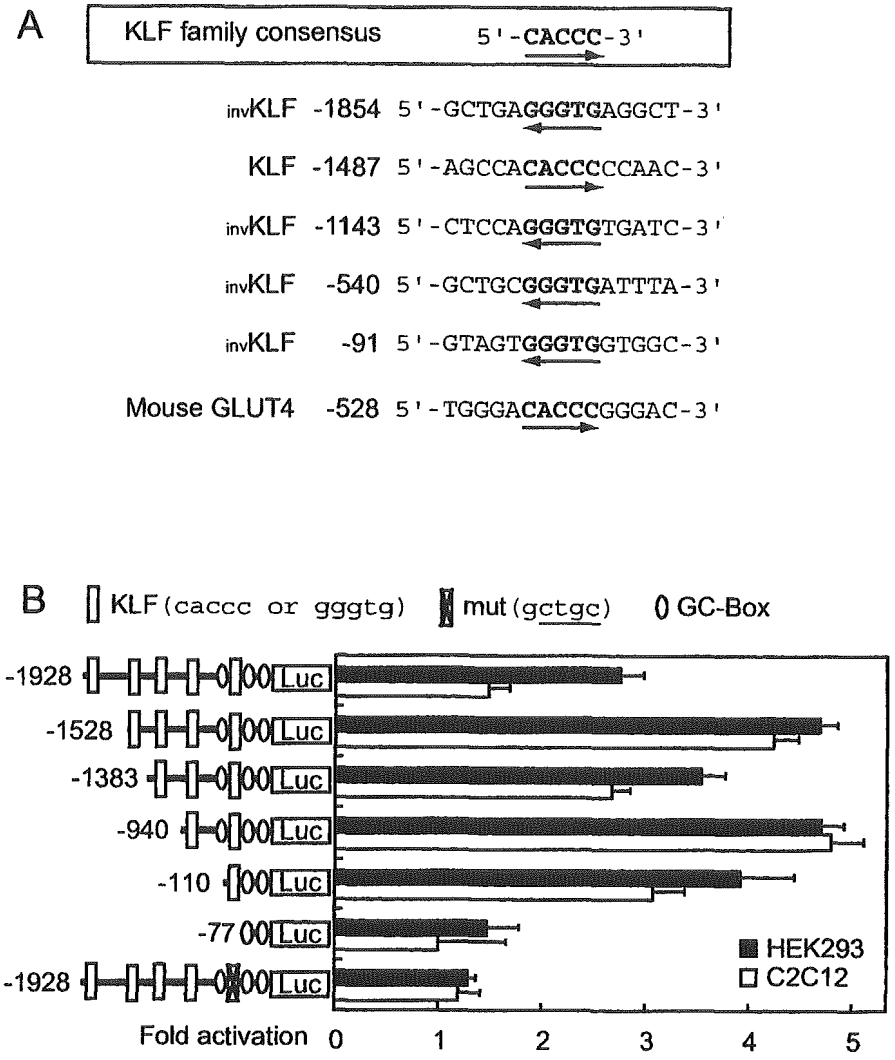

FIG. 4. **KLF15 motifs in the *AcecS2* promoter.** *A*, alignment of five KLF motifs in the *AceCS2* promoter. The sequences of potential KLF motifs at −1854, −1487, −1143, −540, and −91 and their surroundings in the AceCS2 promoter are compared with KLF15 binding sequence in the mouse *GLUT4* promoter. The KLF motifs in the inverted orientation are labeled with inv. *B*, localization of KLF15 responsive element by progressive deletion and mutation analyses. On day 0, HEK293 cells were seeded at a density of 2×10^4 cells/well in 24-well plates. On day 1, the cells were transfected with 0.8 μg of the indicated AceCS2-luciferase reporter and 0.1 μg of pRL-TK together with 0.01 μg of pCMV-KLF15 or pcDNA3.1. On day 2, the cells were harvested, and firefly and *Renilla* luciferase activities were determined as described under "Experimental Procedures." The -fold activation (luciferase activity co-transfected with pCMV-KLF15 *versus* pcDNA3.1) is shown. The *error bars* represent mean ± S.E. of triplicate incubations.

II, and PDK4 mRNAs were determined by quantitative real time PCR. As shown in Fig. 1*A*, insulin treatment did not alter the levels of AceCS2 mRNA, whereas those of hexokinase II and PDK4 were, respectively, induced and reduced by insulin treatment. Similarly, the levels of AceCS2 mRNA in human skeletal myotubes were not altered (Fig. 1*B*), suggesting that fasting-induced *AceCS2* gene expression is not directly dependent on insulin action.

5′-Flanking Region of the Mouse AceCS2 Gene—To determine the mechanism regulating fasting-induced expression of the *AceCS2* gene, we initially isolated and characterized the 5′-flanking region of the mouse *AceCS2* gene. Approximately 2.4-kb upstream of the translation initiation ATG was isolated by PCR (see "Experimental Procedures") and was sequenced (Fig. 2*A*). The transcription initiation sites were determined by 5′-RACE experiments on poly(A)$^+$ RNA from mouse skeletal muscle using an AceCS2 transcript-specific primer (see "Experimental Procedures"). Sequence analysis of the 5′-RACE products revealed that the *AceCS2* gene has multiple transcription start sites: two major points at −23 and −28 and four minor points at −12, −17, −19, and −53 (Fig. 2*A*); the A of the translation initiation ATG of the gene is designated +1.

Trans-activation of AceCS2 Promoter by KLF15—Potential elements for various transcription factors were identified by computer-assisted search using AliBaba2.1 (www.gene-regulation.com/pub/programs/alibaba2/index.html) and TFSEARCH (www.cbrc.jp/research/db/TFSEARCHJ.html). As summarized in Fig. 2*B*, the 5′-upstream of the most 5′ transcription initiation site (−53) consists of potential sites for MyoD (−1509, −1379, and −698), IRS (−1509 and −1243), c-Ets-1 (−1435 and −1409), HNF1 (−802), MEF2 (−261), and KLF (−1854, −1487, −1143, −540, and −91). There are three GC-boxes located at −65, −76, and −132.

To determine the effects of these transcription factors, the genomic DNA fragment containing the 5′-flanking region (−2347) was ligated with the firefly luciferase gene in pGL3 basic to create pAceCS2(2347). This promoter-reporter was transiently transfected into non-muscle HEK293 cells along with the indicated transcription factor(s) listed in Fig. 3. All the expression plasmids used in this study were well characterized by the original investigators from whom we obtained. All the plasmids were confirmed by restriction enzyme digestions and partial sequencing. For the expression of AFX and FKHR, since they contain a FLAG epitope tag, we performed immunoblot analyses using an anti-FLAG antibody and confirmed that protein were expressed properly (data not shown). For the other transcription (co-) factors, we have performed real time PCR analysis, because of the unavailability of their antibodies. The transfection efficiencies were also examined by *Renilla* luciferase activities as described under "Experimental Procedure." As shown in Fig. 3, among 13 transcription factors tested, only KLF15 trans-activated the *AceCS2* promoter re-

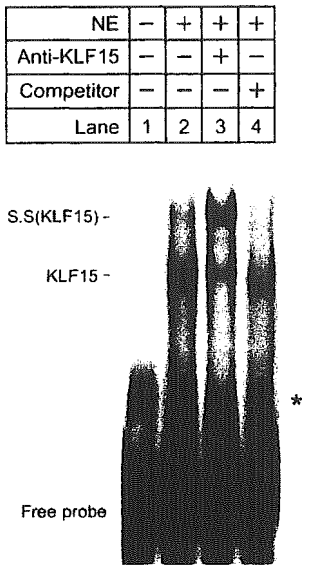

FIG. 5. **EMSA of KLF15-binding to the *AceCS2* gene promoter.** Nuclear extracts were prepared from C2C12 cells stably expressing KLF15 and incubated with labeled double-stranded oligonucleotide containing a putative KLF binding site (at −91), followed by EMSA as described under "Experimental Procedures." The KLF15-specific shifted band and the supershifted band (*S.S*) specific to the KLF15 antibody are indicated on the *left*. Nonspecific band is denoted by an *asterisk*.

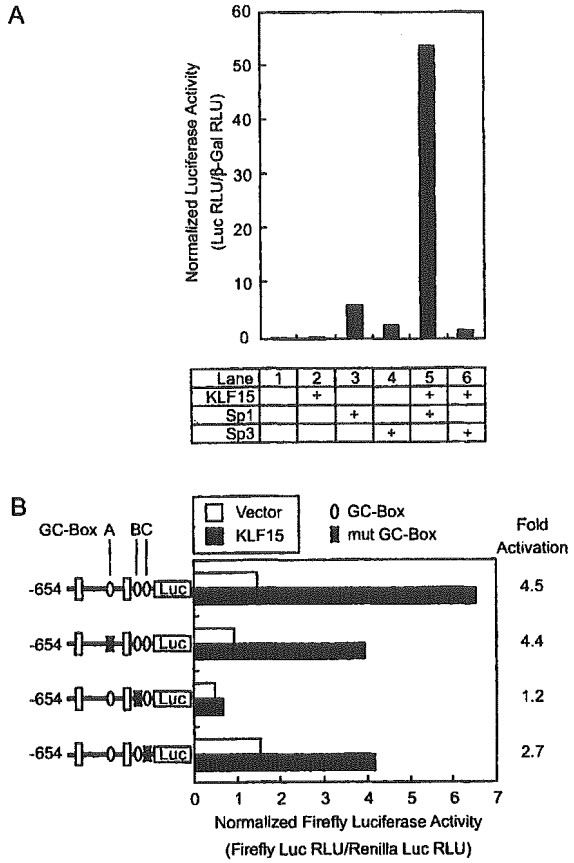

FIG. 6. **KLF15 and Sp1 cooperate to induce *AceCS2* promoter activity.** *A*, KLF15 functions synergistically with Sp1. On day 0, SL2 cells were plated at a density of 2×10^5 cells/well in 24-well plates. On day 1, the cells were transfected with 0.5 μg of pAceCS2 (654) and 0.1 μg of pPac-β-gal (internal reference encoding the β-galactosidase gene) together with 0.01 μg of the indicated plasmid. On day 2, the cells were harvested, and luciferase activity was measured and normalized to β-galactosidase activity. Each value represents the average of duplicate incubations. *B*, mutation analyses of three GC-boxes in *AceCS2* promoter. pAceCS2(654) and its mutants, in which each GC-box was mutated, were constructed as described under "Experimental Procedures." On day 0, 2×10^4 cells/well of HEK293 cells were set up in 24-well plates. On day 1, the cells were transfected with 0.8 μg of the indicated luciferase reporter construct and 0.1 μg of pRL-TK together with 0.01 μg of pCMV-KLF15 or pcDNA3.1. On day 2, the cells were harvested, and firefly luciferase activity was measured and normalized to *Renilla* luciferase activity. The -fold activation (luciferase activity co-transfected with pCMV-KLF15 *versus* pcDNA3.1) is shown. Each value represents the average of duplicate incubations.

porter activities: ~5.5-fold induction was detected by co-transfection with KLF15. Other KLFs, KLF6 or KLF9 had almost no effects.

KLF15 is known to form a heterodimer complex with MEF2A and the resulting complex synergistically induces the transcription of *GLUT4* gene (23). On the other hand, MEF2 family of transcription factors MEF2A, 2B, 2C, and 2D had no synergistic effects on the AceCS2 reporter activities when coupled with KLF15. Each of the MEF2 family of transcription factors, MEF2A-2D, alone had almost no effects.

We also examined the effects of peroxisome proliferator-activated receptor γ co-activator 1 (PGC-1α) in the absence or presence of KLF15 or MEF2 family of transcription factors, MEF2A-2D. Neither PGC-1α alone, PGC-1α in the presence of KLF15, nor PGC-1α with each of the MEF2 family of transcription factors had stimulatory effects on the promoter reporter activities. The forkhead box transcription factors FKHR (also known as FOXO1) (24, 25) and AFX (FOXO4) (11) are involved in insulin-responsive gene activation. Thus we examined the effects of FKHR and AFX on the *AceCS2* promoter activities. As a positive control experiment, we transfected AFX and FKHR together with a reporter-luciferase under the control of three copies of insulin responsive sequence (IRS) in tandem. This configuration, which is based on the *IGFBP-1* promoter/enhancer elements, gave rise to abundant luciferase activity (Fig. 3, *inset*) (11). Consistent with the lack of insulin-dependence, neither FKHR nor AFX had stimulatory effects on the *AceCS2* promoter in the absence or presence of KLF15.

Other factors MyoD, cEts-1, HNF1α, and HNF1β in the absence or presence of KLF15 were inactive. Although these transcription factors were not active in this reporter assay and we cannot exclude the possibility of their significance in the regulation of *AceCS2* gene *in vivo*, these data indicate that KLF15 plays a key role in the trans-activation of the *AceCS2* gene.

Crucial KLF Binding Site in the AceCS2 Promoter—There are five potential KLF15 binding sites within 2.4-kb region of the *AceCS2* promoter. Fig. 4*A* compares the sequences of five potential KLF15 sites and their surroundings in the *AceCS2* promoter with that present in the *GLUT4* gene. Although four of the five KLF15 sites are inversely orientated, all the five sequences contain an identical sequence of CACCC that is specifically bound by KLF15 (23) and other KLF family of transcription factors (26–28).

To determine the most crucial KLF binding site, a series of 5′-deletions was introduced into the promoter region. Deletion of the sequence from −1928 to −110 did not change the trans-activation by KLF15 (Fig. 4*B*). A further deletion to −77 resulted in almost complete loss of induction by KLF15. Similar results were obtained using a myogenic line, C2C12 cells. Furthermore, the reporter construct containing a mutated KLF binding site lacked inducible activity. Similarly, in the context of pAceCS2 (−1928), the mutation in the most proximal KLF binding site lacked the inducible activity, indicating that the most proximal KLF site is a curtail site for the trans-activation of the *AceCS2* gene by KLF15.

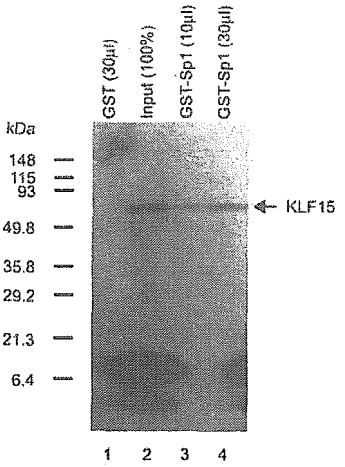

FIG. 7. **KLF15 interacts with Sp1 *in vitro*.** Glutathione beads bound with *E. coli* cell-expressed GST-Sp1 (10 and 30 μl) or GST (30 μl) were incubated with *in vitro* transcribed/translated ^{35}S-labeled KLF15 at 4 °C for 1 h. After washing extensively, the proteins bound on the beads were analyzed by SDS-PAGE and visualized by autoradiography.

TABLE II
Quantitative real time PCR of various KLF transcripts in skeletal muscle of fasted and fed mice

Total RNAs from skeletal muscles of fasted (48 h) or fed mice were subjected to quantitative real-time PCR as described under "Experimental Procedures." Cyclophilin mRNA was used as the invariant control. Values represent the relative amount of mRNA in skeletal muscle of fasted mice relative to that of fed mice, which is arbitrarily defined as 1. The values are mean of three mice.

Krüppel-like factor	Fold induction (Fasted/Fed)
KLF1	2.11
KLF2	1.69
KLF3	2.28
KLF4	1.88
KLF5	2.62
KLF6	6.88
KLF7	1.24
KLF8	1.69
KLF9	5.50
KLF10	2.29
KLF11	3.72
KLF12	1.29
KLF13	1.86
KLF14	1.67
KLF15	27.9
KLF16	1.19

EMSA of KLF15-Binding Site in the AceCS2 Promoter—To determine whether KLF15 is capable of binding to the most proximal KLF site of the *AceCS2* promoter, we performed EMSA using labeled probe (double-stranded 36-mer corresponding −70 to −105) with the nuclear extracts from C2C12 cells stably expressing KLF15. As shown in Fig. 5, the nuclear extracts containing KLF15 produced a single band of DNA-protein complex. This complex was specific as it can be competed by unlabeled probe. Furthermore, this complex can be supershifted with an antibody against KLF15, indicating that KLF15 is able to bind to the most proximal KLF site to the transcription start point of the *AceCS2* gene.

Synergistic Transcriptional Activation by KLF15 and Sp1—In contrast to the synergic transcriptional activation of the *GLUT4* gene by KLF15 and MEF2 (23), none of MEF family transcription factors in combination with KLF15 synergistically trans-activated the *AceCS2* promoter (see Fig. 3). The proximity of the KLF15 binding site and GC boxes raised the possibility that KLF15 and Sp1 may function in a coordinated manner to induce the *AceCS2* promoter. To assess this possibility, we performed co-transfection studies using Sp-null *Drosophila* SL2 cells. As shown in Fig. 6*A*, we observed that the combination of KLF15 and Sp1 resulted in a synergistic activation of the *AceCS2* promoter (*lanes 1*, *3*, and *5*): ~10-fold by comparison to Sp1 alone. Although Sp3 recognizes the same sequence as Sp1, and Sp3 alone trans-activated the *AceCS2* promoter (Fig. 6*A*, *lane 4*), the combination of KLF15 and Sp3 did not synergistically induce the *AceCS2* promoter (Fig. 6*A*, *lane 6*).

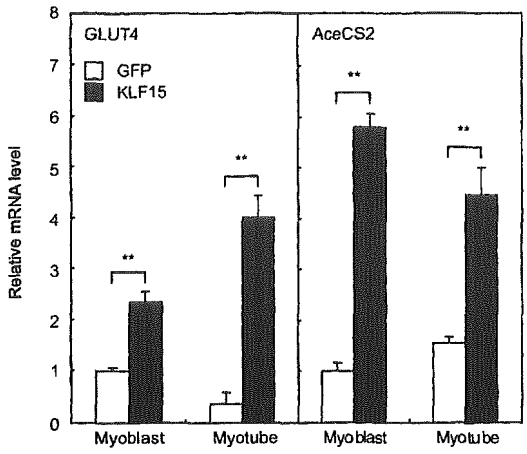

FIG. 8. **Induction of GLUT4 and AceCS2 transcripts in C2C12 cells stably expressing KLF15.** On day 0, C2C12 stably expressing KLF15 (C2C12/KLF15) and GFP (C2C12/GFP) were individually plated in 6-well plates at a density of 1×10^5 cells/well and cultured in medium A. On day 2, the cells were either harvested (myoblasts) for RNA extraction, or induced to differentiate into myotubes by incubating in medium B for an additional 7 days. Medium was changed every other day. On day 9, myotubes were harvested for RNA extraction. Total RNA from myoblasts and myotubes were subjected to quantitative real time PCR with specific primers for GLUT4 (*A*) or AceCS2 (*B*). Cyclophilin was used as the invariant control. Values represent the amount of mRNA relative to that in C2C12/GFP myoblasts, which is arbitrarily defined as 1. The *error bars* represent mean ± S.E. of triplicate incubations.

There are three GC-boxes, termed as GC-boxes A, B, and C, within 100 bases upstream of the most 5′ transcriptional initiation site (−53) of the *AceCS2* gene. To further define the role of these GC-boxes in the synergistic trans-activation with KLF15, we introduced mutations in each of the three GC-boxes in pAceCS (654) (see "Experimental Procedures" and Fig. 6*B*). For this co-transfection experiment with these mutant promoter-reporters, we used HEK293 cells. As shown in Fig. 6*B*, mutations in GC-box B in the *AceCS2* promoter almost completely abolished the trans-activation by KLF15, while other mutants containing mutated GC-boxes A or C retained the trans-activation activity by KLF15. These data indicate that GC-box B, located 8 bases downstream of the most crucial KLF15 site, is the most important site in the synergistic trans-activation of the *AceCS2* gene by KLF15 and Sp1.

To determine whether KLF15 and Sp1 interact directly to activate the *AceCS2* promoter, we carried out GST pull-down assays. As shown in Fig. 7, *in vitro* transcribed/translated ^{35}S-labeled KLF15 was bound with GST-Sp1 fusion protein, but not with GST, indicating that KLF15 interacts with Sp1 *in vitro*.

Induction of KLF15 Transcripts in Skeletal Muscle of Fasted Animals—To test whether fasting induces KLF15 expression, like the *AceCS2* gene, we carried out quantitative real time RT-PCR analysis of KLF transcripts. As shown in Table II, 48 h fasting robustly induced the KLF15 transcripts in the skeletal muscle of mice: the levels of KLF15 transcripts in fasted animals were ~28-fold higher than those in fed animals. Together

with the trans-activation of the *AceCS2* promoter, it is suggested that this fasting-induced AceCS2 expression is largely contributed by KLF15.

Overexpression of KLF15 in C2C12 Myogenic Cells Induces the Expression of AceCS2 Transcripts—We next examined the effects of KLF15 overexpression on the levels of AceCS2 transcripts in C2C12 myogenic cells. C2C12/KLF15 and C2C12/GFP cells were cultured in non-differentiation medium (medium A) or differentiation medium (medium B) and the levels of AceCS2 transcripts were determined by quantitative real time RT-PCR. As shown in Fig. 8, KLF15 overexpression induced the levels of AceCS2 transcripts by severalfold both in myoblasts and in myotubes, indicating that *AceCS2* gene expression *in vivo* is indeed induced by KLF15.

DISCUSSION

In the current study, we provide evidence that fasting-induced transcriptional activation of the *AceCS2* gene in the skeletal muscle is contributed largely by a unique transcription factor KLF15. KLF15 is a recently characterized member of the Sp1-like/KLF family and regulates *GLUT4* gene expression in both adipose and muscle cells (23). Consistent with the induction of AceCS2 transcripts, the levels of KLF15 transcripts in the skeletal muscle are also robustly induced by fasting. Together with the trans-activation of the *AceCS2* promoter by KLF15, this co-induction of KLF15 by fasting may indicate that fasting-induced AceCS2 transcription is largely contributed by KLF15.

KLF15 is a member of the Sp1-like/KLF family, a family of highly related zinc-finger DNA binding proteins that are important regulators of cellular development, differentiation, and activation (29). It is highly expressed in the liver, kidney, adipose tissue, heart, and skeletal muscle (23, 30). Gray *et al.* demonstrated that KLF15 specifically induces the expression of the insulin-sensitive glucose transporter GLUT4 and glucose uptake in 3T3-L1 cells. It was also shown that KLF15 directly interacts with MEF2, a known activator of the *GLUT4* promoter, and activates the *GLUT4* promoter in a synergistic manner. On the other hand, our current data show that KLF15 in combination with a general transcription factor Sp1, synergistically activates the *AceCS2* promoter. In this context, it is interesting to note that the two AceCSs require Sp1 for their trans-activation; activation of the *AceCS1* gene is synergistically regulated by SREBPs and Sp1 (3).

Fasting-induced gene expression is of current interest. Especially, the induction of hepatic gluconeogenic genes during prolonged fasting or starvation is important for survival. Recently, Puigserver *et al.* (25) showed that insulin-regulated hepatic induction of gluconeogenic genes is mediated through interaction of FKHR and PGC-1α. In the skeletal muscle, genes involved in fatty acid oxidation and PDK4 are up-regulated during fasting in order to suppress glucose utilization (4, 5). We recently showed evidence that the PPARδ together with PGC-1α mediates the induction of genes involved in fatty acid transport, β-oxidation, and mitochondrial respiration in the skeletal muscle (31). The gene expression profile induced by PPARδ is very similar to those induced by fasting in the skeletal muscle (4, 5). Therefore, PPARδ together with PGC-1α may play a part in the muscle expression of genes induced by fasting.

Our current data provide evidence for a unique role of KLF15 in the activation of fasting-induced genes in the skeletal muscle. In the skeletal muscle, KLF15 is the most abundant KLF and its induction by fasting is most potent among 16 KLFs. To our knowledge, AceCS2 and GLUT4 are the only known targets for KLF15. It is therefore important to identify target genes driven by KLF15. These studies are currently in progress.

Acknowledgments—We thank Drs. Akiyoshi Fukamizu, Ryuji Hiramatsu, Takashi Minami, G. P. Nolan, Eric N. Olson, Bruce M, Spiegelman, Guntram Suske, and Kazuya Yamagata for plasmid constructs, Toshio Kitamura for a retroviral packaging cell line, Kazuya Yamada for helpful discussion, Aoi Uchida and Yasuyo Urashima for technical assistance.

REFERENCES

1. Fujino, T., Kondo, J., Ishikawa, M., Morikawa, K., and Yamamoto, T. T. (2001) *J. Biol. Chem.* **276,** 11420–11426
2. Luong, A., Hannah, V. C., Brown, M. S., and Goldstein, J. L. (2000) *J. Biol. Chem.* **275,** 26458–26466
3. Ikeda, Y., Yamamoto, J., Okamura, M., Fujino, T., Takahashi, S., Takeuchi, K., Osborne, T. F., Yamamoto, T. T., Ito, S., and Sakai, J. (2001) *J. Biol. Chem.* **276,** 34259–34269
4. Jagoe, R. T., Lecker, S. H., Gomes, M., and Goldberg, A. L. (2002) *FASEB J.* **16,** 1697–1712
5. Pilegaard, H., Saltin, B., and Neufer, P. D. (2003) *Diabetes* **52,** 657–662
6. Yechoor, V. K., Patti, M.-E., Saccone, R., and Kahn, C. R. (2002) *Proc. Natl. Acad. Sci. U. S. A.* **99,** 10587–10592
7. Naya, F. J., Black, B. L., Wu, H., Bassel-Duby, R., Richardson, J. A., Hill, J. A., and Olson, E. N. (2002) *Nat. Med.* **8,** 1303–1309
8. Molkentin, J. D., Black, B. L., Martin, J. F., and Olson, E. N. (1995) *Cell* **83,** 1125–1136
9. Puigserver, P., Wu, Z., Park, C. W., Graves, R., Wright, M., and Spiegelman, B. M. (1998) *Cell* **92,** 829–839
10. Hatta, M., Daitoku, H., Matsuzaki, H., Deyama, Y., Yoshimura, Y., Suzuki, K., Matsumoto, A., and Fukamizu, A. (2002) *Int. J. Mol. Med.* **9,** 147–152
11. Fukuoka, M., Daitoku, H., Hatta, M., Matsuzaki, H., Umemura, S., and Fukamizu, A. (2003) *Int. J. Mol. Med.* **12,** 503–508
12. Minami, T., Tachibana, K., Imanishi, T., and Doi, T. (1998) *Eur. J. Biochem.* **258,** 879–889
13. Yamagata, K., Yang, Q., Yamamoto, K., Iwahashi, H., Miyagawa, J., Okita, K., Yoshiuchi, I., Miyazaki, J., Noguchi, T., Nakajima, H., Namba, M., Hanafusa, T., and Matsuzawa, Y. (1998) *Diabetes* **47,** 1231–1235
14. Yoshiuchi, I., Yamagata, K., Zhu, Q., Tamada, I., Takahashi, Y., Onigata, K., Takeda, J., Miyagawa, J., and Matsuzawa, Y. (2002) *Diabetologia* **45,** 154–155
15. Sakai, J., Rawson, R. B., Espenshade, P. J., Cheng, D., Seegmiller, A. C., Goldstein, J. L., and Brown, M. S. (1998) *Mol. Cell* **2,** 505–514
16. Morita, S., Kojima, T., and Kitamura, T. (2000) *Gene Therap.* **7,** 1063–1066
17. Pear, W., Nolan, G., Scott, M., and Baltimore, D. (1993) *Proc. Natl. Acad. Sci. U. S. A.* **90,** 8392–8396
18. Applied Biosystems (2001) *User Bulletin No. 2, Rev B,* Applied Biosystems, Forster City, CA
19. O'Brien, R. M., and Granner, D. K. (1996) *Physiol. Rev.* **76,** 1109–1161
20. Hall, R. K., Yamasaki, T., Kucera, T., Waltner-Law, M., O'Brien, R., and Granner, D. K. (2000) *J. Biol. Chem.* **275,** 30169–30175
21. Zhang, J., Ou, J., Bashmakov, Y., Horton, J. D., Brown, M. S., and Goldstein, J. L. (2001) *Proc. Natl. Acad. Sci. U. S. A.* **98,** 3756–3761
22. Kishida, K., Shimomura, I., Kondo, H., Kuriyama, H., Makino, Y., Nishizawa, H., Maeda, N., Matsuda, M., Ouchi, N., Kihara, S., Kurachi, Y., Funahashi, T., and Matsuzawa, Y. (2001) *J. Biol. Chem.* **276,** 36251–36260
23. Gray, S., Feinberg, M. W., Hull, S., Kuo, C. T., Watanabe, M., Sen-Banerjee, S., DePina, A., Haspel, R., and Jain, M. K. (2002) *J. Biol. Chem.* **277,** 34322–34328
24. Furuyama, T., Kitayama, K., Yamashita, H., and Mori, N. (2003) *Biochem. J.* **375,** 365–371
25. Puigserver, P., Rhee, J., Donovan, J., Walkey, C. J., Yoon, J. C., Oriente, F., Kitamura, Y., Altomonte, J., Dong, H., Accili, D., and Spiegelman, B. M. (2003) *Nature* **423,** 550–555
26. Nuez, B., Michalovich, D., Bygrave, A., Ploemacher, R., and Grosveld, F. (1995) *Nature* **375,** 316–318
27. Perkins, A. C., Sharpe, A. H., and Orkin, S. H. (1995) *Nature* **375,** 318–322
28. Vliet, J. v., Turner, J., and Crossley, M. (2000) *Nucleic Acids Res.* **28,** 1955–1962
29. Kaczynski, J., Cook, T., and Urrutia, R. (2003) *Genome Biol.* **4,** 206
30. Uchida, S., Tanaka, Y., Ito, H., Saitoh-Ohara, F., Inazawa, J., Yokoyama, K. K., Sasaki, S., and Marumo, F. (2000) *Mol. Cell. Biol.* **20,** 7319–7331
31. Tanaka, T., Yamamoto, J., Iwasaki, S., Asaba, H., Hamura, H., Ikeda, Y., Watanabe, M., Magoori, K., Ioka, R. X., Tachibana, K., Watanabe, Y., Uchiyama, Y., Sumi, K., Iguchi, H., Ito, S., Doi, T., Hamakubo, T., Naito, M., Auwerx, J., Yanagisawa, M., Kodama, T., and Sakai, J. (2003) *Proc. Natl. Acad. Sci. U. S. A.* **23,** 15924–15929

J Hum Genet (2004) 49:622–628
DOI 10.1007/s10038-004-0198-4

ORIGINAL ARTICLE

Tadao Iwasaki · Sadao Takahashi · Mitsuaki Ishihara
Masafumi Takahashi · Uichi Ikeda
Kazuyuki Shimada · Takahiro Fujino
Tokuo T. Yamamoto · Hiroaki Hattori · Mitsuru Emi

The important role for βVLDLs binding at the fourth cysteine of first ligand-binding domain in the low-density lipoprotein receptor

Received: 14 July 2004 / Accepted: 5 August 2004 / Published online: 1 October 2004

Abstract The low-density lipoprotein (LDL) receptor (LDLR) is a crucial role for binding and uptaking apolipoprotein (apo) B-containing lipoproteins, such as very-low-density lipoprotein (VLDL), intermediate-density lipoprotein (IDL), and LDL. The defect function of the LDLR causes familial hypercholesterolemia (FH), the phenotype of which is elevated plasma cholesterol and premature coronary heart disease (CHD). In the present study, we characterize the role of the cysteine residue of the ligand-binding domain of the LDLR. The mutant LDLR protein of cysteine for serine at codon 25 (25S-LDLR) was expressed in Chinese hamster ovary (CHO) cell line, *ldl*-A7. By Western blot analysis, the 25S-LDLR was detected with monoclonal antibody IgG-12D10, which reacts with the linker site of the LDLR but not with IgG-C7, which reacts with the NH_2 terminus of the receptor. The 25S-LDLR bound LDL similarly to the wild-type LDLR, but the rate of uptake of LDL by the mutant receptor was only about half of that by the wild-type receptor. In contrast, the 25S-LDLR bound and internalized β VLDL more avidly than LDL. These results suggest that the fourth cysteine residue of the first ligand-binding domain of the LDLR might be important for the internalization of atherogenic lipoproteins by vascular cells despite reduced LDL uptake, leading to atherosclerosis and premature cardiovascular disease.

Keywords Familial hypercholesterolemia · Low-density lipoprotein receptor · Mutation · Ischemic heart disease · Atherosclerosis

Abbreviations *FH* Familial hypercholesterolemia · *LDL* Low-density lipoprotein · *VLDL* Very-low-density lipoprotein · *LDLR* Low-density lipoprotein receptor · *VR* Very-low-density lipoprotein receptor · *ER2* Apolipoprotein E receptor 2 · *IHD* Ischemic heart disease · *DiI* 3,3′-Dioctadecylindocarbocyanine iodide

T. Iwasaki · M. Ishihara · H. Hattori
Department of Advanced Medical Technology and Development, BML, Inc., Saitama, Japan

S. Takahashi
The Third Department of Internal Medicine, School of Medicine, Fukui University, Fukui, Japan

M. Takahashi · U. Ikeda
Department of Organ Regeneration, Shinshu University Graduate School of Medicine, Matsumoto, Japan

K. Shimada
Division of Cardiology, Department of Medicine, Jichi Medical School, Tochigi, Japan

T. Fujino · T. T. Yamamoto
Gene Research Center, Tohoku University, Sendai, Japan

M. Emi (✉)
Department of Molecular Biology, Institute of Gerontology, Nippon Medical University, 1-396 Kosugi-cho, Nakahara-ku, Kawasaki 211-8533, Japan
E-mail: memi@nms.ac.jp
Tel.: +81-44-7335230
Fax: +81-44-7335192

Introduction

Familial hypercholesterolemia (FH) is an autosomal-dominant inherited disease caused by mutations in the low-density lipoprotein (LDL) receptor (LDLR) gene. Heterozygous FH has a population frequency of one in 500 (Goldstein et al. 1995). The clinical features of FH are an elevated plasma cholesterol due to impaired clearance of plasma LDL, the presence of xanthomas, and increased risk of coronary heart disease (CHD) as a consequence of premature atherosclerosis (Brown and Goldstein 1986). It is thought that the high incidence of

CHD in FH might be caused by the mechanism out of LDLR because of its functional defect.

The LDLR protein contains five domains, which include a ligand-binding domain, an epidermal growth factor precursor homology domain, an *o*-linked sugar domain, a membrane-spanning domain, and a cytoplasmic tail domain (Goldstein et al. 1995; Russell et al. 1989a). The ligand-binding region of LDLR consists of seven contiguous ligand-binding repeats each approximately 40 amino acids long with a repeat of six cysteine residues (Sudhof et al. 1985). This combination of repeats folds a cluster of conserved negatively charged sequences (Ser-Asp-Glu) with disulfide bond connections (Esser et al. 1988; Russell et al. 1989b; Bieri et al. 1995a) and allows LDLR to bind plasma lipoproteins containing apolipoprotein (apo) B-100 and apoE (Brown and Goldstein 1986; Mahley 1988). The first two ligand-binding repeats (LB1 and LB2) of the human LDLR are autonomously folding domains that contain three disulfide bonds with a Cys(I)-Cys(III), Cys(II)-Cys(V) and Cys(IV)-Cys(VI) connectivity (Bieri et al. 1995a,b). Mutations deleting one of the third to the seventh repeats in the ligand-binding domain of the LDLR result in a marked reduction of LDL binding (Russell et al. 1989b). The LDLR requires calcium ions for the physiologic binding of lipoprotein particles, which is eliminated in the presence of EDTA (Kita et al. 1981). The recognition of the first repeat, LB1, by a conformationally specific monoclonal antibody IgG-C7, is also dependent on the presence of calcium (van Driel et al. 1987). The ligand-binding repeat is thought to function as a protein-binding domain, which interacts with Lys and Arg residues, resembling the positively charged receptor-binding regions of apo B-100 and apoE. Differences in the number and rearrangement of these repeated sequences are thought to be responsible for the diversity of ligands that bind to the LDLR (Hobbs et al. 1990). We have previously reported a mutation at the fourth cysteine of the first ligand-binding domain in the LDLR gene in a homozygous FH patient (Takahashi et al. 2001). In this study, we have generated a mutant protein in CHO cells and examined its functional activity toward lipoproteins.

Materials and methods

Lipoprotein preparation

Human LDL ($d = 1.006$–1.063 g/ml) and rabbit β-very-low-density lipoprotein (VLDL) ($d < 1.006$ g/ml) was prepared by sequential preparative ultracentrifugation as previously described (Kujiraoka et al. 2000; Kosaka et al. 2001). Each lipoprotein (1 mg) was labeled with 1 mg/ml 3,3′-dioctadecylindocarbocyanine iodide (DiI; Molecular Probes, MO) by incubation for 3 h at room temperature (Corsetti et al. 1991), and after ultracentrifugation at the same density, fluorescent-labeled lipoproteins were isolated and exhaustively dialyzed against 150 mmol/l NaCl and 0.24 mmol/l EDTA (pH 7.4). Proteins were measured according to the method of Lowry (Lowry et al. 1951).

Engineering and cloning of human LDLR

The human LDLR cDNA (pLDLR3; ATCC 57004) in the pEF321 vector (Kim et al. 1990) was used as a template for PCR. The mutant cDNA of the LDLR was cloned from peripheral blood lymphocytes of a proband by RT-PCR using a paired primer 5′ complementary forward primer (5′-GACTCTAGACAATTGATGGGGCCCT-GGGGCTGGAAATTGC-3′) and 3′ reverse primer (5′-GACTGCGACCAATTGTCACGCCACGTCATC-CTCCAGACTG-3′) for the C25S mutation of the LDLR; 5′ complementary forward primer (5′-CTGG-GGGTCTTCCTTCTATGGTAGAACTGGCGGCTT-AAGAAC-3′). and 3′ reverse primer (5′-GTTCTTA-AGCCGCCAGTTCTCACCATAGAAGGAAGACC-CCCAG-3′) for the K790X mutation of the LDLR as control. The resultant approximately 500 bp human LDLR fragment was ligated into pBluescript II-SK vector (Stratagen) by digestion with *Xba*I and *Sal*I, and each vector was transformed into chemically competent DH5 cells (Toyobo, Osaka, Japan). The entire LDLR cDNA sequence was sequenced in both directions for three individual clones using an ABI autosequencer (Applied Biosystems, CA, USA). The three clones were found to be identical, and one was selected for further use. The hLDLR plasmid for transfection was amplified in LB culture medium (containing 100 μg/ml ampicillin) and purified using QIAGEN plasmid kits. Isolated plasmid stocks were stored at −20°C.

Generation of stable cell line

Chinese hamster ovary (CHO) cells (*ldl*A7) were co-transfected with hLDLR plasmids of wild and mutant types and pSV2-neo by the calcium phosphate transfection method using a ratio of 19:1 (pEF321-hLDLR:pSV2-neo). Transfected cells were selected using 700 μg/ml G418 (Sigma), and several clones were screened and selected for LDLR expression by a flow-cytometric procedure with antibody IgG-12D10 (Hattori et al. 2002). Each clone was established by two rounds of dilution cloning and identified as the highest protein-expressing clone. Each cell line for wild type and mutant LDLR was maintained under continuous selection using 700 μg/ml of G418 in DMEM/ham's F12 (Nissui Parmaceutical, Tokyo, Japan), 10% heat-inactivated fetal bovine serum, and 0.01% penicillin-streptomycin. The amount of LDLR protein on the surfaces of transfected CHO cells was measured using a specific monoclonal antibody (mAb) against LDLR by flow cytometry, as below.

Measurement of cell-surface LDLR protein and its functional activity by fluorescence-activated cell-sorter (FACS) flow cytometry

The LDLR protein on the cell surface and LDLR functional activity was measured by a flow cytometry, as previously described (Hattori et al. 2002). For the expression of the LDLR in CHO cells, the amount of LDLR protein on the cell surfaces was measured using a specific mAb against the LDLR—IgG-C7 (Amersham Pharmacia Biotech, Buckinghamshire, UK) or IgG-12D10, the latter of which is raised against the synthetic peptide WPQRCRGLYVFQGDSSPC, representing 158–175 amino acid residues of the human LDLR (Kosaka et al. 2001). The binding and uptake of lipoproteins in cells was measured using DiI-labeled LDL (DiI-LDL) or DiI-βVLDL. All results were expressed as mean intensity of fluorescence (MIF) after subtracting the background values (MIF typically less than 50) obtained with murine IgGs or in the presence of 2 mM EGTA or excess 50-fold unlabeled LDL or βVLDL.

Protein isolation and Western blot analysis

Cell protein was prepared according to a standard method (Kosaka et al. 2001) and quantified using BCA protein assay kit (Pierce, CA, USA). Total cell protein (1 μg) was subjected to sodium dodecyl sulfate (SDS)-polyacrylamide gel electrophoresis (PAGE) with 5–20% slab gels containing 0.1% SDS. Immunoblotting was performed, as previously described (Kujiraoka et al. 2000).

Results

Expression of mutant LDLR protein in CHO cells

To analyze the function of the mutant LDLR, wild-type mutant 25S and 790X human LDLR cDNA were separately transfected into *ldl*-A7 cells, a line of mutant CHO cells that do not express LDLRs (Kingsley and Krieger 1984). The transfection was carried out with pSV2-Neo, and G418-resistant clones were selected. Several clones of each transfected CHO cell were established, and the representative results below shown in the transfected cells expressed the receptor equally determined by the Western blotting and flowcytomeric procedure.

The expression levels of cell-surface LDLR were examined in cell lysates (10 μg protein) from each transfectant by SDS-PAGE using monoclonal antibodies specific for the LDLR IgG-12D10, which reacts with the linker site between repeats 4 and 5 of the ligand-binding domain (Kosaka et al. 2001), and IgG-C7, which reacts with amino-acid residues 1–17 of the NH_2 terminus of the LDLR (Beisiegel et al. 1981). The wild-type and 790X LDLR protein were detected equally with IgG-C7 and IgG-12D10 while 25S-LDLR was detected only with IgG-12D10 (Fig. 1).

The cell-surface LDLR protein in the transfected cells was also examined by the flowcytometric procedure. The expression level of membrane-associated LDLR in the mutant 25S-LDLR and 790X-LDLR CHO cell was 86% and 92% of that of the wild type by IgG-12D10, respectively, and 3.9% and 104% by IgG-C7 (Fig. 2).

Functional activity of mutant LDLR

The binding and uptake activity of lipoproteins in mutant LDLR cells was analyzed using DiI-LDL and DiI-βVLDL in a flow cytometer. The binding and uptake activity of DiI-LDL were 91% and 48% for 25S-LDLR and 118% and 39% for 790X-LDLR, respectively (Fig. 3). The binding and uptake activity of DiI-βVLDL were 71% and 92% for 25S-LDLR and 54% and 44% for 790X-LDLR, respectively (Fig. 4). The internalization indexes (the MIF value internalized divided by the MIF value bound on the surface) for LDL and βVLDL were 3.3 and 2.6 for the wild type, 1.7 and 3.2 for 25S-LDLR, and 1.1 and 2.0 for 790X-LDLR, respectively (Fig. 5).

Discussion

LDLR plays an essential role in lipoprotein metabolism, and defective function of the receptor causes an autosomal dominant disease, FH. Homozygous FH is rare, but heterozygous FH has a frequency of about one in 500 (Goldstein et al. 1995). FH patients have frequently

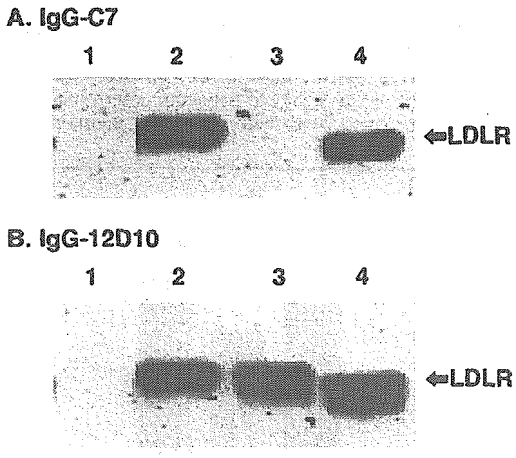

Fig. 1 The expression of the low-density lipoprotein receptor (LDLR) protein in the transfectant by Western blotting. Membrane protein (10 μg) from each transfected Chinese hamster ovary (CHO) cell was subjected to sodium dodecyl sulfate (SDS)-polyacrylamide gel electrophoresis (PAGE). The immunoblotting was carried out using monoclonal antibody **a** IgG-C7 or **b** IgG-12D10. *Lane 1*, CHO/Neo; *lane 2*, wild-type LDLR; *lane 3*, 25S-LDLR; *lane 4*, 790X-LDLR

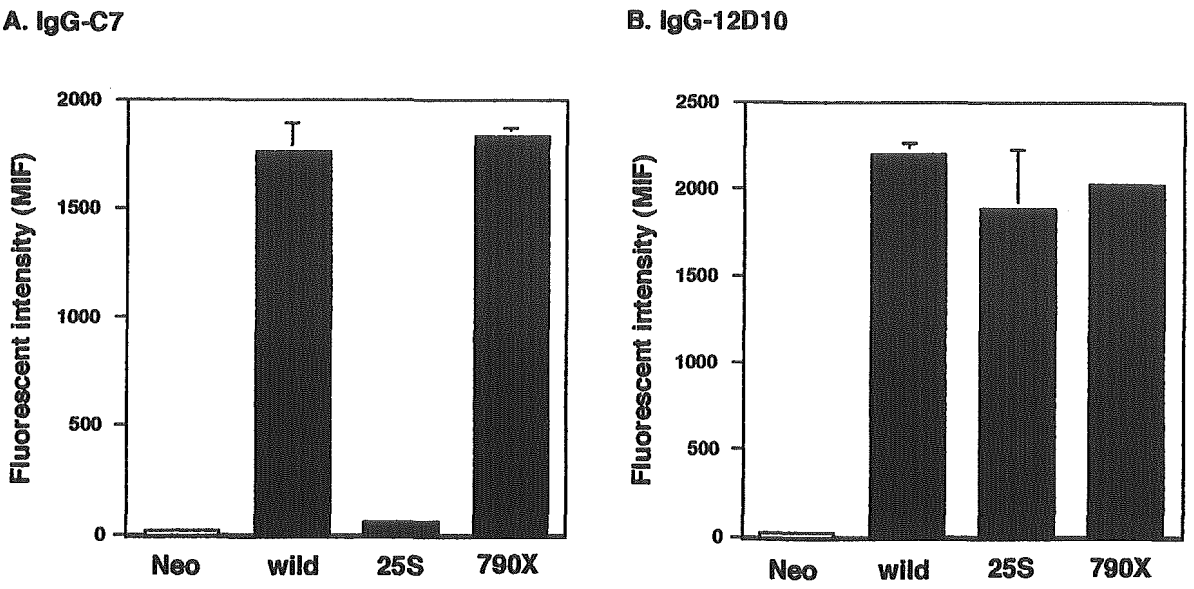

Fig. 2 Cell-surface low-density lipoprotein receptor (LDLR) protein in transfected Chinese hamster ovary (CHO) cells, quantified in a fluorescence-activated cell-sorter (FACS) flow cytometer using monoclonal antibody **a** IgG-C7 or **b** IgG-12D10. Results are the mean fluorescent intensities in transfected cells after subtraction of nonspecific bound IgG (obtained by incubating cells with mouse control IgG). Results represent the mean ± SD of triplicate determinations. The experiment was performed twice with essentially identical results

progressed to CHD, and it is believed that a mutant receptor does not contribute the pathogenesis of CHD. Most of the LDLR gene mutations were identified by a substitution of nucleotide, and the functional defects of LDLR protein were not well characterized. In this study, we have characterized the function of the first ligand-binding domain of the LDLR protein.

By Western blot analysis and flowcytometric procedure, the mutant 25S-LDLR protein expressed in CHO cells, which is a substitution of serine for cysteine at the fourth cysteine (codon 25) of the first cysteine-rich repeat in the ligand-binding domain, was detected with IgG-12D10, which reacts with the linker site between repeats 4 and 5 of the ligand-binding domain of the LDLR (Kosaka et al. 2001) but not with IgG-C7, which reacts with amino-acid residues 1–17 of the NH_2 terminus of the LDLR (Beisiegel et al. 1981). These results indicated that the mutant protein was expressed normally on the cell surface. The substitution at the fourth cysteine of the first ligand-binding domain would create a conformational change of the ligand-binding domain, resulting in no recognition by IgG-C7. Yamamoto et al. (1984) and Goldstein et al. (1985) have previously shown that most of the cysteines in the LDLR form disulfide

Fig. 3 Binding and uptake of DiI-labeled low-density lipoprotein (DiI-LDL) by low-density lipoprotein receptors (LDLR). Results are the mean intensity of fluorescence (MIF) in transfected Chinese hamster ovary (CHO) cells after subtraction of nonspecific binding or uptake of DiI-LDL in the presence of excess unlabeled LDL. Results represent the mean ± SD of triplicate determinations. The experiment was performed twice with essentially identical results

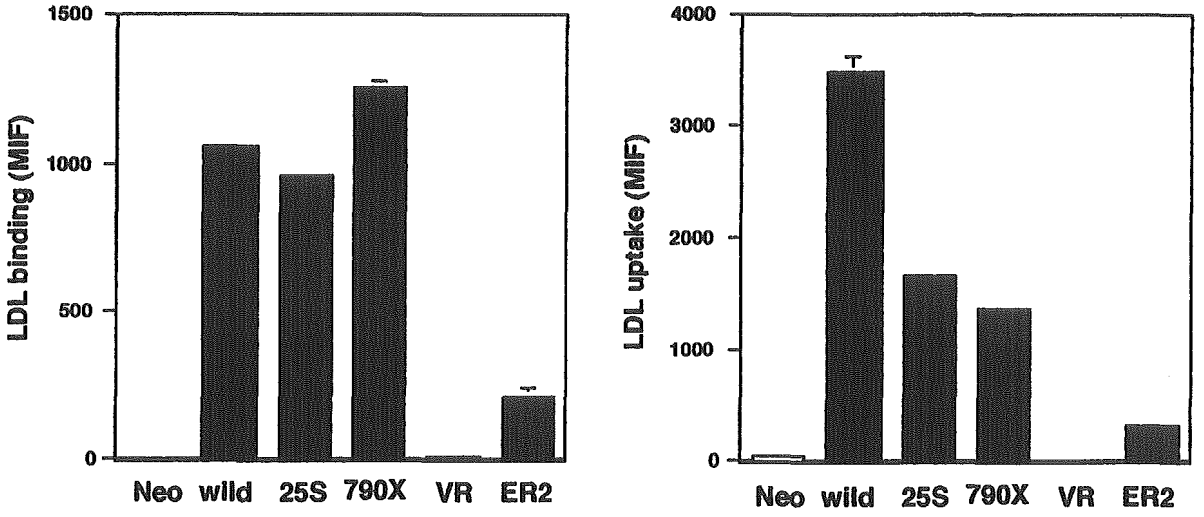

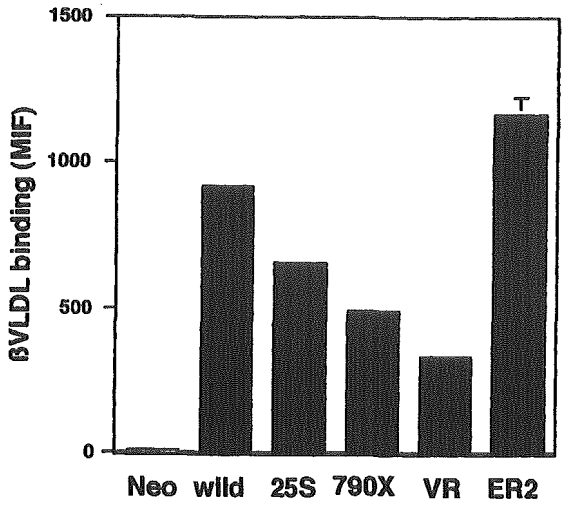

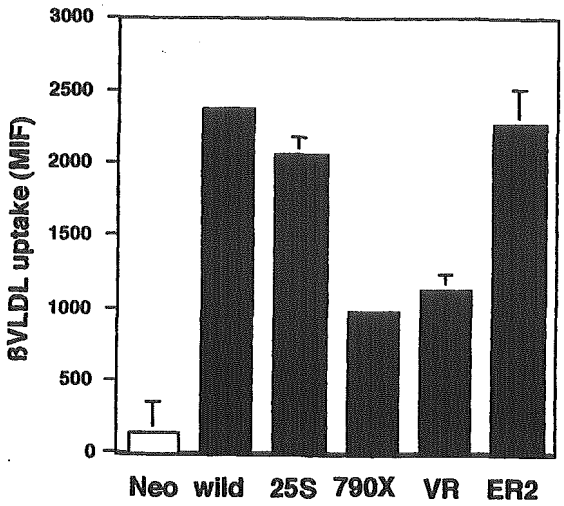

Fig. 4 Binding and uptake of DiI-labeled β very-[low-density-lipoprotein (DiI-βVLDL) by the low-density lipoprotein receptor (LDLR). Results are the mean intensity of fluorescence (MIF) in transfected Chinese hamster ovary (CHO) cells after subtraction of nonspecific binding or uptake of DiI-βVLDL in the presence of excess unlabeled βVLDL. Results represent the mean ± SD of triplicate determinations. The experiment was performed twice with essentially identical results

bridges. The disulfide bond connections between Cys(I) and Cys(III), Cys(IV) and Cys(VI), and Cys(II) and Cys(V) in the first cysteine-rich repeat fold a cluster of negatively charged residues, including the conserved Ser-Asp-Glu sequence, in the first ligand-binding repeat of the LDLR (Bieri et al. 1995a). Moreover, IgG-C7 binds only to the calcium complex of the repeat (Bieri et al. 1998). Therefore, the fourth cysteine residue may have an important function for the ability to bind calcium in the first ligand-binding repeat.

The LDL binding activity of the 25S-LDLR was similar to that of the wild-type LDLR, but the uptake of LDL was only about half of that mediated by the wild type. In contrast, the binding of βVLDL was slightly decreased (70% of the wild type), and βVLDL uptake was almost the same as that by the wild type. Mutational analysis of the ligand-binding domain of the LDLR revealed that mutations of the first ligand-binding repeat, Cys6Ala and Cys18Ala, which are the first and third cysteines, had no defect in the binding of antibody IgG-15C8 against the first repeat of the ligand-binding domain (residues 2–42) or of LDL and βVLDL (Esser et al. 1988). The deletion of the first cysteine-rich repeat also had no defect in the binding of LDL or βVLDL. Together with their report and the results in the present study, the alteration of disulfide bond connection has no affect on the ligand binding of the receptor. It has been

Fig. 5 Internalization index of low-density lipoprotein (LDL) and β very-low-density lipoprotein (βVLDL) by the low-density lipoprotein receptor (LDLR). Internalization index was calculated by dividing mean intensity fluorescence (MIF) internalized fluorescence-labeled lipoproteins by that of surface-bound lipoproteins. The result shown are representative of two independent experiments